

# Multiscale Engine Simulations using a Coupling of 0-D/1-D Model with a 3-D Combustion Code

J. Bohbot, M. Miche, P. Pacaud and A. Benkenida

Institut français du pétrole, IFP, 1-4, avenue de Bois-Préau, 92852 Rueil-Malmaison Cedex - France  
e-mail: julien.bohbot@ifp.fr - marjorie.miche@ifp.fr - pierre.pacaud@ifp.fr - adlene.benkenida@ifp.fr

**Résumé — Simulations multi-échelles de moteur à combustion interne par couplage de modèle 0D/1D avec un code de combustion 3D** — La réduction des émissions polluantes et de la consommation de carburants des moteurs à combustion interne nécessite le développement de nouveaux concepts utilisant des modes de combustion non conventionnels (e.g. HCCI, CAI). Pour réduire les temps de développement et évaluer les bénéfices attendus de ces prototypes, la simulation système est couramment utilisée et permet de simuler le comportement de l'ensemble du moteur et de tous les sous-systèmes qui le composent (Turbo, circuit EGR, etc.). Cette approche système 0D/1D utilise des modèles physiques phénoménologiques nécessitant des bases de données expérimentales afin de fixer les valeurs des différents paramètres des modèles. Toutefois, ces données ne sont pas toujours disponibles. Pour résoudre ce problème, une solution consiste à combiner les approches systèmes et la simulation 3D. En effet, la simulation système peut être utilisée pour simuler la boucle d'air et l'injection de carburant afin de fournir les données nécessaires à la simulation 3D de la chambre de combustion. Cette utilisation conjointe de la simulation système et de la simulation 3D permet d'améliorer la précision des simulations moteurs. Pour cela, deux méthodologies ont été développées et sont décrites dans ce papier. La première méthode est basée sur un prétraitement de simulation 3D afin de générer une cartographie numérique et expérimentale de la combustion qui peut être utilisée par les modèles phénoménologiques 0D. La deuxième méthodologie utilise un couplage temporel direct entre le simulateur 0D/1D et le code de combustion 3D. Ces deux méthodologies de couplage sont décrites et appliquées sur des configurations moteurs afin de démontrer l'intérêt de ces simulations couplées.

**Abstract — Multiscale Engine Simulations using a Coupling of 0-D/1-D Model with a 3-D Combustion Code** – Requirements for the reduction of both pollutant emissions and fuel consumption mean that there is a need to design of new engine concepts (e.g. HCCI, CAI, etc.). To reduce the time of the development loop for these concepts, 1D approaches can be used to simulate whole-engine behaviour. These approaches are based on phenomenological models that need to be fitted to experimental data. However these data are not always available. One way to solve this problem consists in combining 1D and 3D approaches: 1D simulations are used in the gas exchange system or for the fuel injection system and provide necessary inputs (e.g. volumetric efficiency, thermodynamic state, mixture composition, mass flow rate, etc.) for 3D simulations which are used in the combustion chamber to ensure an accurate description of the combustion process (especially pollutant emissions). This strategy allows us to obtain much more information and should improve the predictivity of the simulation. Two different approaches to carry out this coupling have been developed, the first one is based on the pre-processing of the 3D numerical results to generate combustion maps and the second one used a direct temporal coupling between the 1D and the 3D codes. The two methods are described in this paper. We also report on the relevant engine simulations which were carried out to demonstrate the capabilities of the two coupled approaches.

## INTRODUCTION

Stringent emissions regulations for diesel and gasoline engines mean that innovative technologies need to be used in order to reduce consumption and pollutant emissions. This is a real challenge that implies the management of complex interacting dynamic systems such as engines. In the case of spark ignition (SI) engines, downsizing combined with turbocharging creates new possibilities to improve efficiency at low loads while increasing the power. The two basic boost pressure actuators used on current turbocharged SI engines are the throttle and the waste gate. Optimization of the turbocharged engine for consumption, performance, driving comfort and pollutant emissions requires an appropriate engine control management strategy during transient operating conditions. For a complete engine system, this optimization is complex and needs a large number of simulations to develop the relevant control strategies. For Diesel engines, advanced fuel injection strategies, including multiple pilot and post injections, can be used to reach the required levels of emissions reduction, while maintaining the advantage of high thermal efficiency of a diesel engine. The development of the Common Rail (CR) fuel injection system allows more flexibility and accuracy in controlling the injection parameters and the combustion process in order to meet performance and emissions goals. The CR system applies a constant fuel pressure in the rail that is common for all cylinders. However, many researchers report a drop in the injection pressure and injection-to-injection variations when multiple injection strategies are employed [1-4]. These variations are attributed to injector dynamics, due to the needle motion and pressure waves occurring in the system. That leads to varying injection rates, which can affect the combustion and emissions formation processes, particularly NOX and soot. Typical Computational Fluid Dynamics (CFD) models for the in-cylinder processes in an engine are not able to capture these variations, since the exact injection rates are not known.

1D calculations are generally used to simulate the complex behaviour of the whole engine system (fuel injection system, gas exchange system, turbocharger, etc.). These 1D models can handle real time simulations for transient engine evolutions and can be used to develop relevant control strategies. 1D simulations are highly flexible and can be adapted for the complete range of operation points. However, they use phenomenological models and are not always predictive. These models contain several empirical parameters that need to be fitted with experimental data. 1D simulations can also be used to give initial (trapped mass) and boundary conditions (wall temperature) needed for the 3D calculations.

3D Computational Fluid Dynamics (CFD) calculations are used to investigate physical phenomena where 3D flow effects prevail. Optimization of the geometry of complex engine components (such as intake and exhaust systems and combustion chamber) requires the use of 3D calculations.

Combustion and pollutant emission predictions require 3D simulations to take into account the fuel/air mixing process in the combustion chamber, the internal aerodynamics, the heterogeneous fuel distribution and the chemical processes in the cylinder. All these 3D effects cannot be evaluated with 1D models alone. However, it should be noted that 3D simulations focus on a single component of the whole engine (the cylinder) without the dynamic interaction with the other components of the system.

As part of the virtual engine development, previous work has focused on linking 1D simulations with 3D calculations. In order to improve the predictability of CFD models, a coupling between the engine system (air loop and injection system) and the in-cylinder processes has to be performed. Previous work on 1-D/3-D coupling focuses on the gas dynamics of the intake system. Sinclair *et al.* [7] developed a direct 1-D/3-D coupling model to compute the gas exchange system of a turbocharged DI-diesel engine. They treated the intake manifold and ports as a single 3-D model while the rest of the engine was modelled by a system of 1-D components. They developed a 1-D/3-D coupling interface and obtained encouraging results. Their work shows that 3-D modelling of a single component can be used in a full 1-D system using appropriate 1-D/3-D interface processing. Similar coupling approaches have been followed by Borghi *et al.* [8], Riegler and Bargende [9] and Wehr *et al.* [10], who have developed 3-D CFD models for the intake manifold, coupled with 1-D engine models.

This paper highlights the development of two different coupling methods between a whole 1D engine system and a 3D combustion code. The first method consists of the use of IFP-C3D combustion code to replace or supplement the experimental data of the combustion process needed for the IFP-ENGINE 1D engine simulation. The main difference between this approach and the second approaches is that, in order to keep the CPU performance of the 1D simulation, we exclude a direct 1D/3D coupling. The second method as in [7-10] is to model a single component with a 3D modelling and to use 1D modelling for the rest of the engine. We have chosen to model the combustion with 3D combustion modelling. Indeed, combustion phenomena are mainly driven by the 3D flow effects (fuel/air mixture, turbulence, flame propagation, spray) and 1D models cannot be sufficiently accurate to simulate these processes.

The primary goal of this paper is to demonstrate the two methodologies and the feasibility of these coupling approaches. In the last part of this paper, engine simulations are presented using the coupling methods. First, a transient load simulation is performed using the standard IFP-ENGINE Wiebe's law model [22] with a hybrid combustion map (numerical and experimental). Simulation results are compared to bench results and demonstrate the advantage of the coupling approach. Secondly, the direct coupling is used to compute a 4-cylinder turbocharged gasoline direct injection

engine and a Direct Injection Diesel engine. Numerical results are compared with experimental data to evaluate the 1D/3D coupled simulations with encouraging results for future development.

## 1 THE IFP-ENGINE SIMULATION CODE

The IFP-ENGINE simulation tools are developed under the LMS Imagine.Lab AMESim platform and consist of a 1-D library, IFP-ENGINE allowing the simulation of a complete virtual engine, and of a 3-dimensional combustion code IFP-C3D that can be used for in-cylinder spray and combustion simulations. These two parts are briefly described in this section.

### 1.1 The IFP-ENGINE Library

The IFP-ENGINE library allows the simulation of a complete virtual engine using a characteristic time-scale of the order of the crankshaft angle. A variety of elements are available to build representative models for engine components, such as twin-scroll turbocharger, gasoline or diesel injectors, etc. Figure 1 shows these IFP-ENGINE components. The library uses an advanced modelling approach to take accurately into account the relevant physical phenomena taking place also in the engine [12].

Concerning the combustion process, a first level of modelling is available with an empirical model based on Wiebe's law [22]. This model is used through a mapping of the combustion phenomena based on experimental cylinder pressure; the coefficients of Wiebe's law are calculated defining a map covering the engine operating conditions.

The second level of modelling is given by efficient phenomenological models. For the spark ignition engines, the CFM-1D model is used [20]. This combustion model is based on the CFM combustion model [16] developed at IFP in the IFP-C3D code, presented in the next section. The coherent flame model (CFM) is a combustion model adapted to the flamelet regime for premixed mixtures. This approach is representative of the premixed flame combustion, which represents the main oxidation mechanism in spark ignition (SI) engines. To calibrate this model, 6 different physical coefficients must be defined to calculate the initialisation of the turbulence, the dissipation of the turbulence, the turbulence mixing scale, the flame wrinkling, the flame initial volume and the tumble value. The first 5 are constant coefficients, while the last one defining the tumble coefficient value can be defined as a function of the volumetric efficiency of the engine. For Diesel engines the Chmela [24] and the Barba [21] based model are available.

The heat transfer in the IFP-ENGINE combustion chamber can be simulated with different models. In this paper, the Woschni model [23] will be used, as it appears to be the more relevant for engine applications [24].

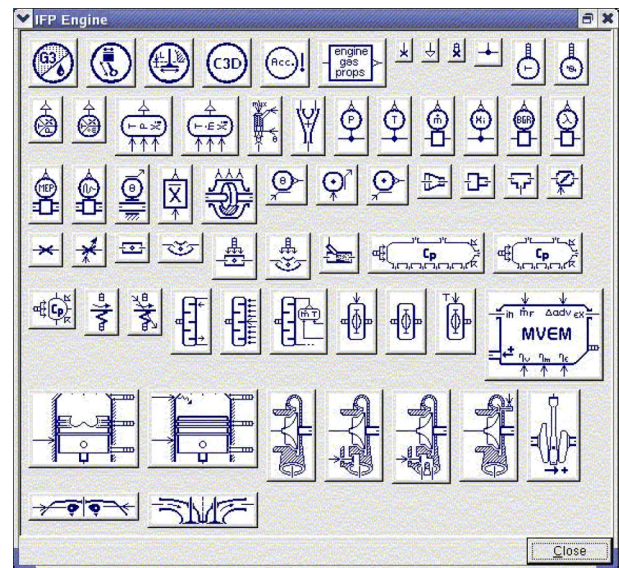


Figure 1  
IFP-ENGINE Library.

### 1.2 IFP-Combustion-Fitting Tool

The purpose of IFP-Combustion-Fitting tool is to obtain the coefficients of Wiebe's law that best match a given cylinder pressure profile. IFP-Combustion-Fitting tool can work with cylinder pressure histories coming from both experimental data and 3D numerical computations. In fact, the user can mix experimental and numerical information in his coefficient map in order to extend the size of the map and its accuracy.

The principle of the optimizer tool consists in translating the information given by the cylinder pressure profile into combustion model coefficients that can be used in an IFP-ENGINE model. In the tool we have developed, we use the classical Wiebe's law of combustion heat release:

$$\frac{dQ_{Wiebe}}{d\theta} = \frac{Q}{\Delta\theta} \cdot a \cdot (f + 1) \cdot y^f \cdot e^{-a \cdot y^{f+1}}$$

$$y = \frac{\theta - \theta_{combustion\_start}}{\Delta\theta}$$

$$\Delta\theta = \theta_{combustion\_end} - \theta_{combustion\_start}$$

For a gasoline engine, 4 parameters must be known to describe the combustion: the combustion starting crank angle, the combustion duration, and two shape coefficients  $a$  and  $f$ . One of the advantages of this tool is that it does not rely on a complete combustion analysis of the cylinder pressure (*i.e.* no need to determine the "experimental" burnt mass

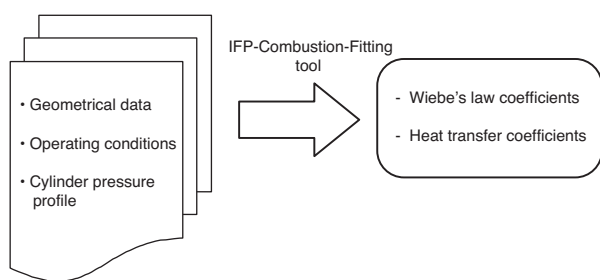


Figure 2  
Optimizer diagram.

fraction by energy balance assumptions). The idea is to perform combustion calculations with an IFP-ENGINE chamber component to find directly the best coefficients of Wiebe's law which fit the cylinder pressure profile. First the beginning and the end of combustion are determined thanks to a basic study of the cylinder pressure profile, then optimization functions are used to match the Wiebe shape coefficients  $a$  and  $f$ . IFP-Combustion-Fitting tool also allows us to optimize the cylinder wall heat transfer coefficients, in order to accurately represent heat loss in the chamber (cf. Fig. 2).

Finally, this tool can automatically deal with several given cylinder pressure profiles; this allows us to rapidly create maps of Wiebe's law coefficients depending on the operating conditions. Typically for a gasoline engine, the parameters of the map are the engine speed, the fuel/air equivalence ratio, the volumetric efficiency, the residual gas ratio, and the spark advance. Since 5D maps are not easy to handle and cannot be taken into account directly in LMS-AMESim for the moment, we have created a specific tool that transforms the 5D data issued from IFP-Combustion-Fitting tool into 3D maps. To do so, we select the three parameters among the five that have the biggest influence on the mapped coefficient variations. A fixed value is also chosen for the two remaining parameters. Then the Wiebe's law coefficient data are organised according to the three main directions chosen and a 3D map is created.

These 3D maps are then used in IFP-ENGINE for the simulation of transient conditions: the combustion at each operating condition is modelled thanks to the value of the Wiebe's law coefficients read on the map.

### 1.3 The IFP-C3D Combustion Code

The IFP-C3D code [13-16] solves the unsteady equations of motion of a turbulent, chemically reactive mixture of gases coupled to a multi-component vaporizing fuel spray. Navier-Stokes equations are solved using a finite volume method extended with an ALE (Arbitrary Lagrangian-Eulerian) scheme. IFP-C3D uses a time-splitting integration and

the temporal integration scheme is largely implicit. Fuel evaporation, break-up, and spray/wall interactions are modelled to simulate the injection. For turbulent combustion the 3-Zone Extended Coherent Flame Model (ECFM3Z), developed at IFP, is used [16, 17]. For Diesel combustion, a full database of auto-ignition delays and reaction rates allows us to compute cold and hot flame ignition [18]. The RNG  $k$ - $\epsilon$  turbulence model [19] with either the Diwakar or Kays and Crawford wall laws are employed, depending on the fuel used (gasoline or diesel).

Species (and tracers), energy and RNG  $k$ - $\epsilon$  turbulent diffusion terms are all implicitly solved by a generic diffusion routine. Parallel optimized linear algebraic libraries developed are used to reverse matrices, rendering parallelization very efficient. The SIMPLE method is applied for solving the coupled pressure-velocity system. All gradient terms used for pressure and the Reynolds stress tensor are parallelly computed. Moreover, efficient preconditioning the pressure matrix significantly reduces the simulation time. The convection terms are explicitly sub-cycled. A second order upwind scheme for scalars and momentum convection is used.

An automatic mesh generator is available in IFP-C3D to create 2-D and 3-D unstructured wedge meshes with periodic boundary conditions. The code is fully integrated in the LMS Imagine.Lab AMESim platform with a user-friendly graphic interface (GUI) and automatic post-processing.

## 2 1D/3D COUPLING APPROACH USING COMBUSTION MAPPING

This 1D/3D coupling approach consists in using a 3D combustion code to generate combustion map when experimental data is not available or is incomplete. The numerical map is calculated using a tool integrated in IFP-ENGINE that automatically performs the IFP-C3D simulation of all the operating conditions specified by the user. The input files needed for IFP-C3D are automatically generated and the calculations sequentially run in an interactive mode (local computing) or in a batch mode (distant supercomputing). Calculated cylinder pressure profile is then used by IFP-Combustion-Fitting tool to automatically compute the Wiebe's law coefficients. Each set of Wiebe's law coefficients defining an operating condition is arranged and added to a map data file. When the numerical map is completed, the user can begin the 1D transient simulation by choosing the relevant combustion mapped data file (cf. Fig. 3).

## 3 1D/3D COUPLING APPROACH BASED ON A DIRECT TEMPORAL METHOD

The development of a direct coupling approach between two different tools requires the definition of the type of data that have to be transferred and the time scale of the synchronisation enforced by the physical system.

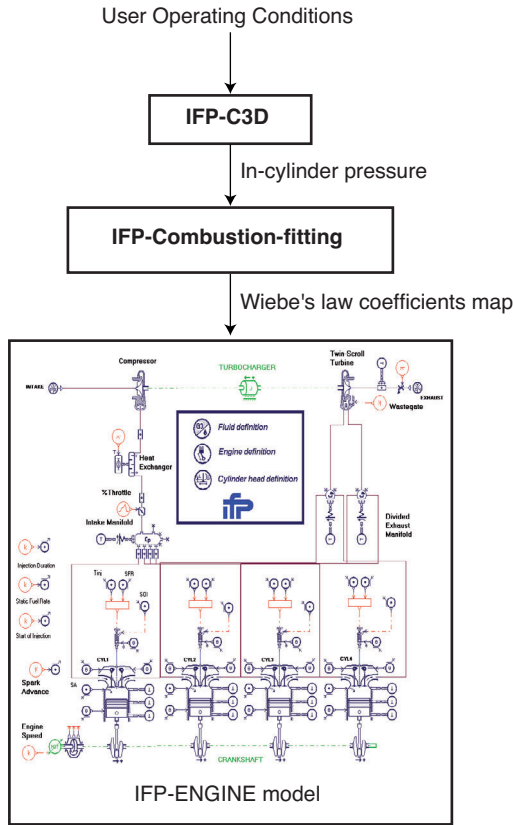


Figure 3  
Coupled methodology.

The main objective of this development is to model with 3D modelling only the combustion process (not the intake, exhaust and direct injection phenomena). An important assumption of this coupling approach is the homogeneous distribution of species in the combustion chamber. The time scale of the synchronisation is the combustion cycle duration (when intake and exhaust valves are closed).

The combustion data needed by the 1D engine system are the species mass consumption and the heat release histories during the combustion cycle. When considering the mass fluxes in the combustion chamber, the total mass flux for each ENGINE gas can be expressed as:

$$\left(\frac{dm_i}{dt}\right)_{Total} = \left(\frac{dm_i}{dt}\right)_{Intake/Exhaust} + \left(\frac{dm_i}{dt}\right)_{Combustion}$$

Then, if the combustion is calculated by IFP-C3D, we have:

$$\left(\frac{dm_i}{dt}\right)_{Combustion} = \left(\frac{dm_i}{dt}\right)_{Combustion}^{C3D}$$

Likewise, if we expressed the internal energy in the combustion chamber:

$$\left(\frac{dU}{dt}\right) = \sum_i \left( \left(\frac{dm_i}{dt}\right)_{Intake/Exhaust} h_i \right) + \frac{dq}{dt} - P \frac{dV}{dt}$$

with  $h_i$  the mass enthalpies,  $dq/dt$  the heat release,  $-PdV/dt$  the pressure forces work.

The total heat release is a combination of the heat release produced by thermal transfer at wall with the heat release produced by the internal combustion.

$$\frac{dq}{dt} = \frac{dq}{dt_{Wall}} + \frac{dq}{dt_{Combustion}}$$

when the intake and exhaust valves are closed, we have:

$$\frac{dq}{dt}^{ENGINE} = \frac{dq^{C3D}}{dt_{Wall}} + \frac{dq^{C3D}}{dt_{Combustion}}$$

When the valves are opened, the Woshni 1D heat transfer model is used to compute the wall heat transfer  $dq/dt_{Wall}$ .

These data have to be transferred from the 3D code to the ENGINE library. However the IFP-ENGINE library uses an assumption of three perfect gases (air, fuel, and burnt gases) whereas IFP-C3D uses a mixture containing 12 gases (fuel,  $O_2$ ,  $N_2$ ,  $CO_2$ ,  $H_2O$ ,  $CO$ ,  $H_2$ ,  $NO$ ,  $OH$ ,  $O$ ,  $H$ ,  $N$ ). To ensure the gases compatibility between the two codes, IFP-C3D computes the mass of the 3 gases needed by IFP-ENGINE using the fuel mass, the  $O_2$  mass and the mass of the species produced by the combustion as described below:

$$\begin{aligned} m_{fuel}^{ENGINE} &= m_{fuel}^{C3D} \\ m_{fresh\ air}^{ENGINE} &= \frac{1}{0.233} m_{O_2}^{C3D} \\ m_{burnt\ gases}^{ENGINE} &= \sum_{i=1..11} m_{specie(i)}^{C3D} - m_{fresh\ air}^{ENGINE} \end{aligned}$$

To complete the direct coupling method, we have defined a temporal staggered algorithm to manage the time lag between the two codes. As shown in Figure 4, the staggered algorithm can be split into three steps.

First, the engine gas exchange system is calculated by IFP-ENGINE. When IFP-ENGINE reaches the Intake Valve Closure (IVC) angle, the calculation is stopped and IFP-C3D starts. Then the 1D library sends the IVC angle, the trapped mass and the mixture composition to the 3D code.

The second step is the 3D combustion calculation using the 1D information as boundary and initial conditions. The 3D calculation is stopped at the Exhaust Valve Opening (EVO) crank angle. Then, IFP-C3D sends the heat release histories (combustion, wall transfer) and the species mass consumption histories to the 1D library.

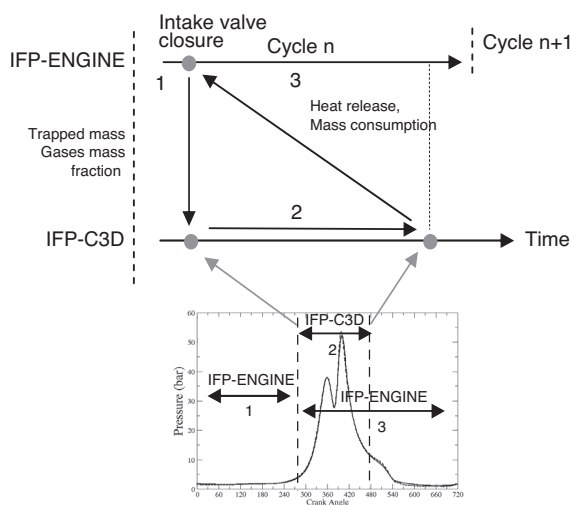


Figure 4  
Staggered coupling algorithm.

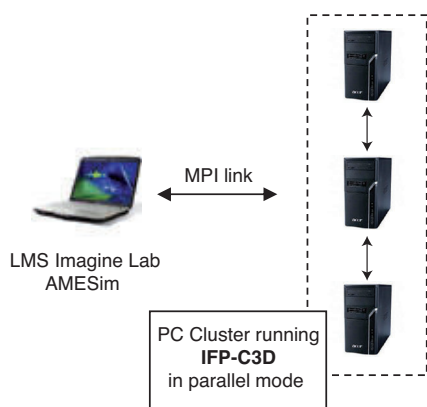


Figure 5  
MPI link between a laptop computer running LMS-AMESim and a Cluster running IFP-C3D.

Finally, IFP-ENGINE restarts the calculation from the IVC to the next engine cycle. During the combustion cycle IFP-ENGINE uses the 3D data to compute at each time step the heat release and the mass consumption.

To manage the coupled calculation, the MPI 2 (Message Passing Interface) paradigm is used to create the link between the two codes. The MPI library is used with a master/slave mode. The master LMS-AMESim/IFP-ENGINE creates an intra-communicator with the IFP-C3D (slave) and can command and communicate with IFP-C3D at any time step. The master/slave mode gives the possibility of managing many slaves to extend the calculation for more than one cylinder but also to use 3-D modelling for other single components (such as air box, 3-D pipe, etc.). Moreover, the CPU

time needed by 3-D calculation and 1-D simulation are very different and generally 3-D calculations have to be performed using a parallel architecture computer with large memory. Homogeneous computer grids can be used with MPI paradigm and LMS-AMESim calculation can be performed on a laptop and 3-D calculations on a PC Cluster (see Fig. 5). This functionality allows the calculation return time to be reduced and makes the coupled calculation return time compatible with industrial requirements.

#### 4 SIMULATION OF TRANSIENT LOAD CONDITIONS USING THE COUPLED METHOD

To assess the validity of the coupling approach based on the 3D combustion mapping, a downsized turbocharged gasoline engine transient load operation was considered. Engine downsizing using turbochargers is one of the major concepts for fuel consumption reduction in SI engines since it gives higher efficiency at low and partial loads. One of the main drawbacks is the turbocharged air path response time which is significantly greater than for naturally aspirated engines. This turbo lag issue is especially observed during transient loads and represents a main concern for downsized engine design.

##### 4.1 Engine Configuration

The main characteristics of the turbocharged gasoline direct injection engine are presented in Table 1.

TABLE 1  
Engine Set up Characteristics

Engine type	RENAULT F5R
Number of cylinders	4
Bore (mm)	82.7
Stroke (mm)	93
Compression ratio	10.56 : 1
Length of connecting rod (mm)	144.5
Engine displacement (L)	2.0
Turbocharger type	Twin-scroll
IVO/IVC	10° CA BTDC / 20° ABDC
EVO/EVC	29° CA BTDC / -9° ABDC

##### 4.2 Engine Model Description

The engine model diagram is presented in Figure 6. The fluid is approximated by 3 gases: fresh air, fuel vapour and burnt gases. The air path consists of pipes, volumes and orifices representing the ducts manifold and piloted air throttle in the intake system.

A heat exchanger is included to simulate compressed gas cooling. The engine block consists of the cylinder head with valves and several combustion chambers. The valve lift and

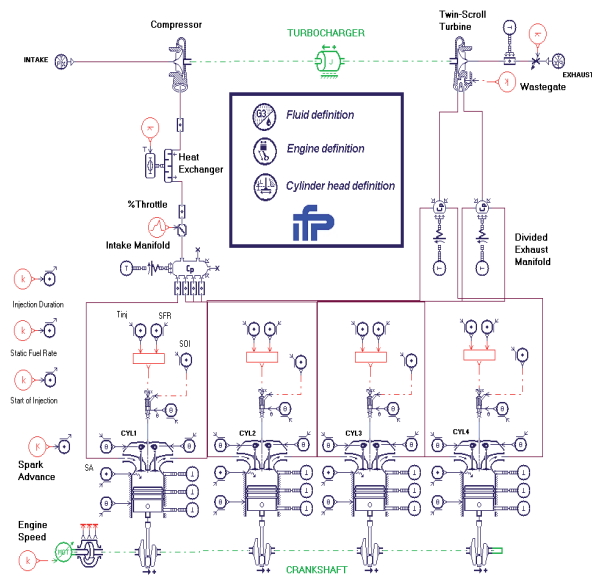


Figure 6  
Turbocharged Gasoline Direct Injection Engine Model.

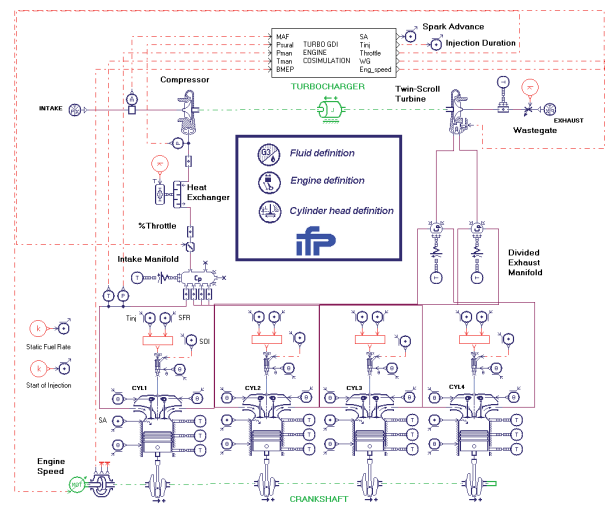


Figure 7  
Co-simulation system for the transient GDI turbo testing.

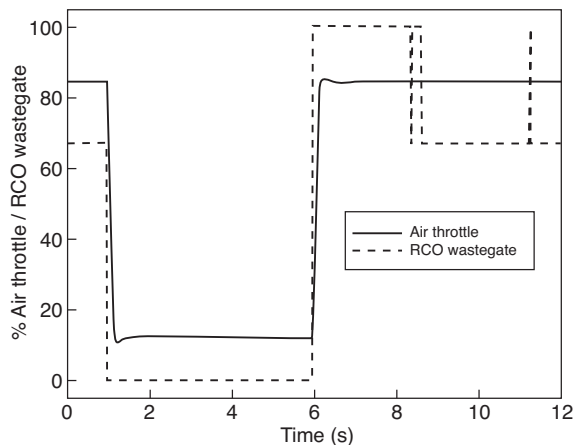


Figure 8  
Air throttle and RCO waste gate trajectories.

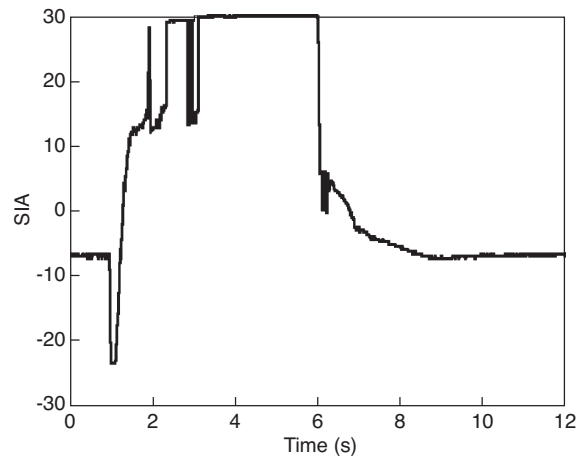


Figure 9  
Spark Advance (SA) trajectory.

permeability characteristics of valve flows are taken into account. Inside the combustion chambers Wiebe’s law predicts combustion behaviour while Woschni’s correlation is used to model heat transfer. The twin-scroll turbocharger model is based on turbo manufacturer maps with additional specific developments in order to take into account gas inertia and divided turbine housing.

### 4.3 Transient Operating Conditions and Validation Set Up

The test case consists of a transient from Wide-Open-Throttle (WOT) to low load conditions followed by a second transient back to WOT. The engine speed is regulated around 1500 rpm. This transient load pattern was achieved on the

engine bench and the actuator trajectories have been recorded. The goal of the validation set up is to test the behaviour of the virtual engine when imposing the same inputs as for the test bench. It means that all the actuator targets are applied to the model with any engine control regulation. This open loop method is a really severe test for the model because any small deviation to real engine test may be emphasised by the absence of engine control.

Figures 8 to 11 present respectively the actuator trajectories: air throttle, RCO waste gate, spark advance, injection duration and engine speed. The test platform consists of a co-simulation between LMS-AMESim and Simulink solvers (Fig. 7). Compared with Figure 6, a co-simulation box, representing the Simulink engine management model, appears on the simulator diagram.

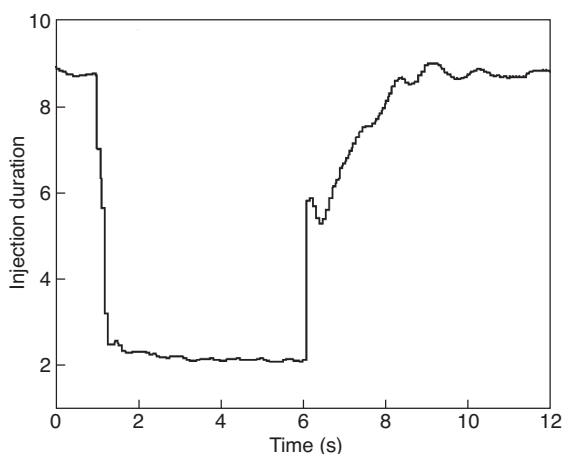


Figure 10  
Injection duration trajectory.

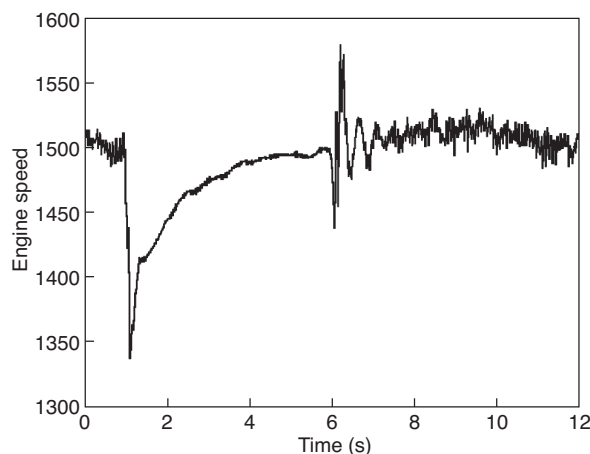


Figure 11  
Engine speed trajectory.

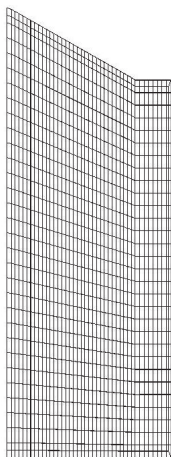


Figure 12  
2D periodic mesh.

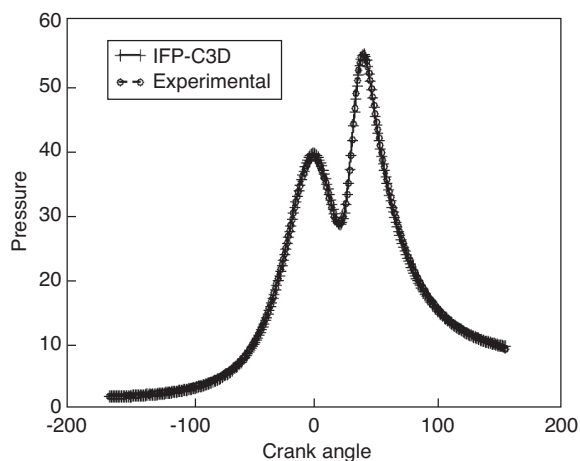


Figure 13  
Comparison of IFP-C3D and experimental in-cylinder pressures.  
Steady test condition 1.

The LMS-AMESim solver is used to compute the engine model behaviour and the actuator trajectories are processed by the Simulink's solver. The two solvers compute independently their respective systems and exchange actuator positions with a fixed communication step interval.

#### 4.4 3D Combustion Calculation

Homogeneous combustion is computed using a 3D mesh with periodic boundary conditions (BC). This mesh is generated by the IFP-C3D internal mesher. The input parameters for the mesh are a set of nodes describing the cylinder head and the piston contours. Figure 12 represents the mesh used for the calculations; it contains 2830 nodes and 1340 cells. For these calculations we used the ECFM3Z combustion model [17] and the turbulent RNG k- $\epsilon$  model [19] to simulate each operating condition. The aerodynamic flow is initialised with a tumble centred in the half chamber. The initial kinetic turbulent energy and turbulent scales were tuned by computing the experimental

in-cylinder conditions listed in Table 2. The turbulent characteristics are then set for the engine and empirical laws give all the turbulent parameters for all our various operating conditions. The initial air mass is computed using the volumetric efficiency defined for each operating condition. We fix the fuel/air equivalence ratio to 1. The residual gas fraction is set to 5%.

Figure 13 presents a comparison between computed cylinder pressure and experimental data for a volumetric efficiency equal to 1.5 and a Spark Advance (SA) equal to  $-9$  (cf. case 1 in *Tab. 2*). The numerical results, very close to the experimental ones, validate the use of the 3D calculation. Aerodynamic parameters are set for this case with a tumble equal to 0.9. Turbulence is initiated with a turbulent kinetic energy equal to  $600 \text{ m}^2 \cdot \text{s}^{-2}$  and a turbulent integral length scale equal to 0.008 m. Figures 14 and 15 present respectively the burnt mass fraction of fuel and the history of the turbulent kinetic energy. The calculated in-cylinder pressures for the different steady state operating conditions presented in Table 2 are shown in Figure 16.

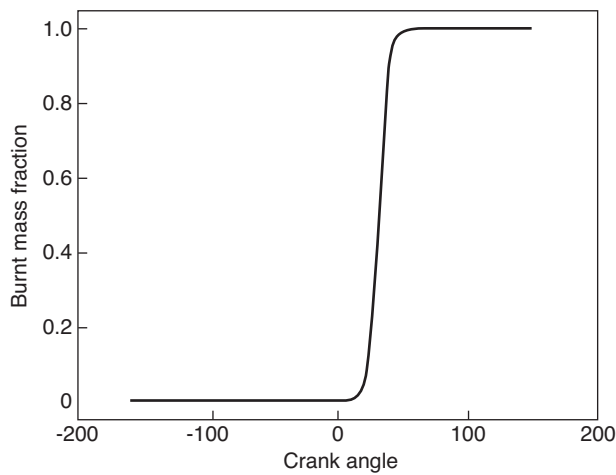


Figure 14  
Fuel burnt mass fraction history.

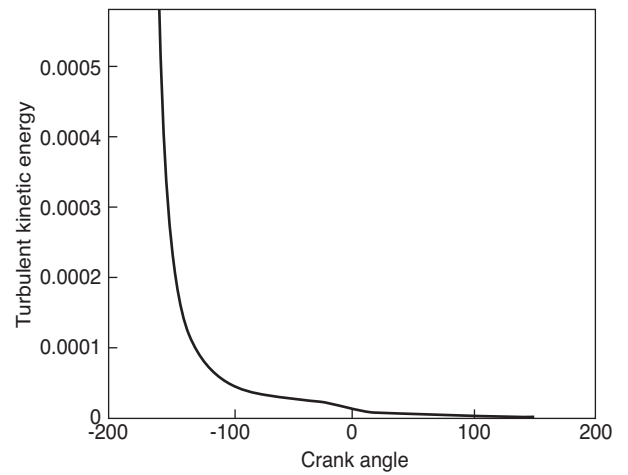


Figure 15  
Turbulent kinetic energy history.

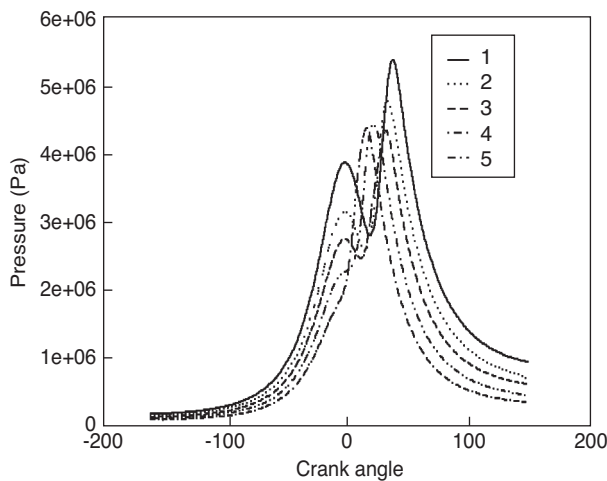


Figure 16  
Computed in-cylinder pressures for all operating conditions listed in Table 2.

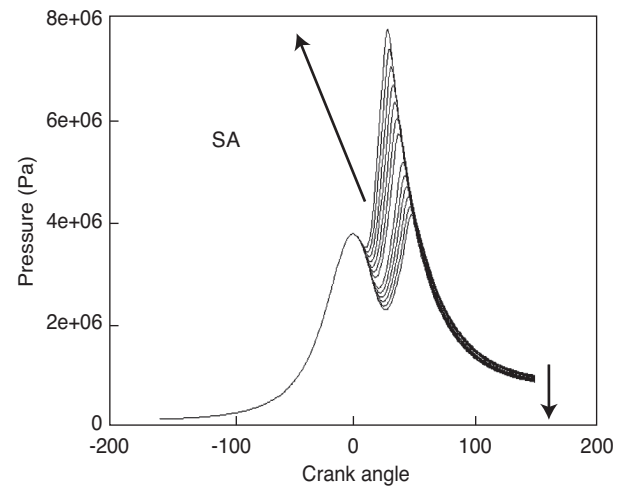


Figure 17  
SA variation, VE = 1.5, BRG = 0.05.

TABLE 2

Experimental in-cylinder conditions

Experimental case	1	2	3	4	5
Volumetric Efficiency (VE)	1.5	1.2	1.	0.8	0.6
Spark Advance (SA)	-9	-6	-3	5	14
Fuel/air Equivalence ratio	1				
Engine speed (rpm)	1500				

#### 4.5 IFP-C3D Calculation of the Numerical Combustion Map

Figure 17 shows the in-cylinder pressure for a variation of the SA obtained with a residual burnt gas fraction fixed at 5% and a volumetric efficiency equal to 1.5. The total CPU time needed to generate the 250 elements of the numerical map is about 60 000 s on a two processor INTEL 2.2 GHz machine.

To represent the transient operating condition described in Figures 8 to 11, we calculated the additional in-cylinder conditions listed in Table 3 to supplement the experimental combustion map listed in Table 2. Calculated cylinder pressure results are used in the IFP-Combustion-Fitting tool to build the numerical combustion map. The numerical map contains 250 sets of Wiebe’s law coefficients. The combustion is computed for various fractions (0%, 5%, 10%, 15%) of residual gases and for a variation of 13 degrees of SA.

As is shown in Figure 17, when the SA increases, the maximum pressure increases and the exhaust pressure decreases. In the same way, Figure 18 presents the in-cylinder pressure computed with IFP-C3D for a burnt residual gases (BRG) variation (0%, 5%, 10%, 15%), a volumetric efficiency equal to 1.5 and a SA equal to -9. The numerical results show that as the BRG increases, the combustion velocity decreases leading to lower combustion and exhaust pressures.

TABLE 3  
IFP-C3D combustion map

Numerical In-cylinder condition set	1	2	3	4	5
Volumetric efficiency	1.5	1.2	1.	0.8	0.6
SA range (every °CA)	[-3, -15]	[0, -12]	[3, -9]	[-1, 11]	[8, 20]
Fuel/air equiv. ratio			1.		
Engine speed (rpm)			1500		
Residual gas range (every 5%)			[0, 15]		

The IFP-C3D pressure results are then processed by the IFP-Combustion-Fitting tool to generate the map of optimal Wiebe's law coefficients. As an example, Figure 19 compares the pressure obtained by IFP-Combustion-Fitting for the first operating condition (VE = 1.5, SA = -9), to the original IFP-C3D results. In this case, the tool generates less than 1% of error in the prediction of Brake Mean Effective Pressure (BMEP).

#### 4.6 IFP-ENGINE Model Transient Load Simulation

After having validated the steady state operating points, the 1D engine model was tested on the transient load operating conditions. Figure 23 shows the variation of the Wiebe's coefficient when we use the combustion map instead of using a constant value when no combustion mapping is used. Figure 20 presents the manifold pressure during the transient for experimental and numerical results. The response of transient air system to both load steps input is well predicted and relative error between experimental and simulated results is about 2.5%. The dynamic behaviour of the air system and combustion during the transient operation is well represented. The decrease of intake pressure during the first transient is well reproduced. At

6 s, the second transient occurs. The throttle is fully opened and the waste gate is fully closed. Rapidly, the intake pressure increases to atmospheric pressure value. Then the compressor speed increases and leads to an increase in boost pressure. As shown in Figure 20, the model intake pressure fits experimental results well during this second transient. These good results on intake pressure for the whole transient pattern demonstrates that the turbocharger inertia is well represented and the accuracy of the air system is well modelled. The supercharging pressure is plotted in Figure 21. During the first transient, the sudden closure of the air throttle may lead the compressor model to pumping conditions. In this engine set up, the turbocharger is fitted out with an expansion valve between the inlet and the outlet of the compressor. This system allows the pumping phenomenon to be avoided by discharging the compressor inlet overpressure. The model reproduces well this aspect and it can be noticed that the model supercharging pressure fits well the experimental results during the whole transient. It reproduces the pressure drop at the throttle opening and increases with a similar behaviour to that of the test-bed. A small deviation can be observed around 5 seconds but the engine is at very low load at this time. The turbocharger is running with a speed lower than 20 000 rpm which is out of the manufacturer's map and increasing the simulation accuracy during this period is difficult.

Finally, Figure 22 presents the effective torque simulated with IFP-ENGINE compared with the control command target. It shows that the engine model gives a realistic response to this control target during the transient with an open loop control based on bench trajectories. One of the main goals of such an engine calculation is to reproduce the turbo response time on intake pressure during load transients. The presented results show very good agreement with bench data on this aspect and the model may be used to prospect strategies in order to reduce the turbo lag effect.

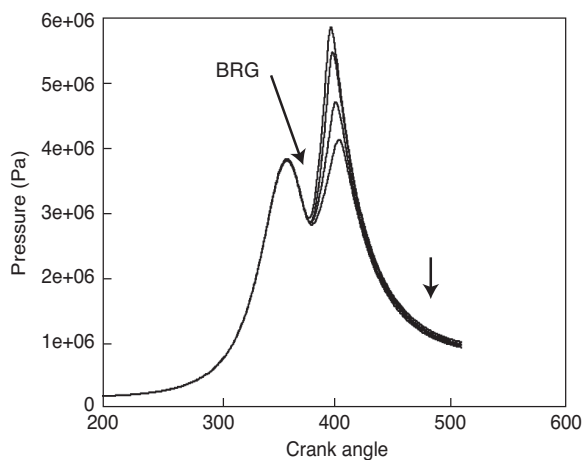


Figure 18  
BRG variation (0%, 5%, 10%, 15%), SA = -9°CA, VE = 1.5.

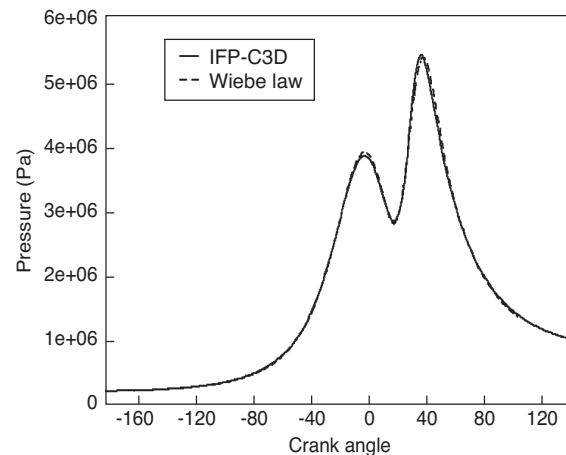


Figure 19  
Combustion Fitting / IFP-C3D average cylinder pressure.

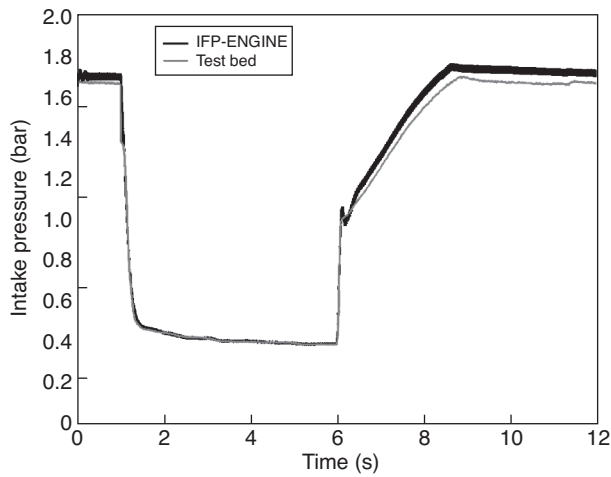


Figure 20  
Intake manifold pressure during transient load.

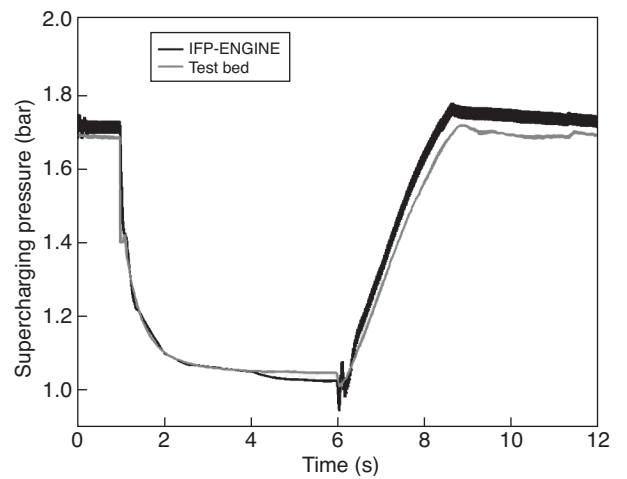


Figure 21  
Supercharging pressure.

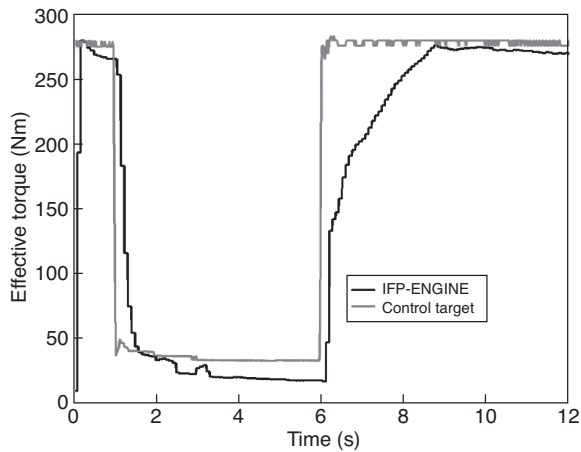


Figure 22  
Effective torque.

### 5 SIMULATION OF A 4-CYLINDER TURBOCHARGED GASOLINE DIRECT INJECTION ENGINE USING THE DIRECT TEMPORAL COUPLING APPROACH

The 1D/3D direct temporal coupling algorithm described previously is used for the modelling of the combustion. The axisymmetric mesh is generated with the internal mesher of IFP-C3D and contains 2000 cells. A two-dimensional (2D) computational mesh of the engine geometry was created, since both the fuel injector and the spark plug are centrally located. Subsequently, the 3D IFP-C3D model was linked with the 1D simulation of the engine systems in order to run a full engine simulation. The total CPU time for one computation on an AMD 2 GHz processor was approximately 3 hours.

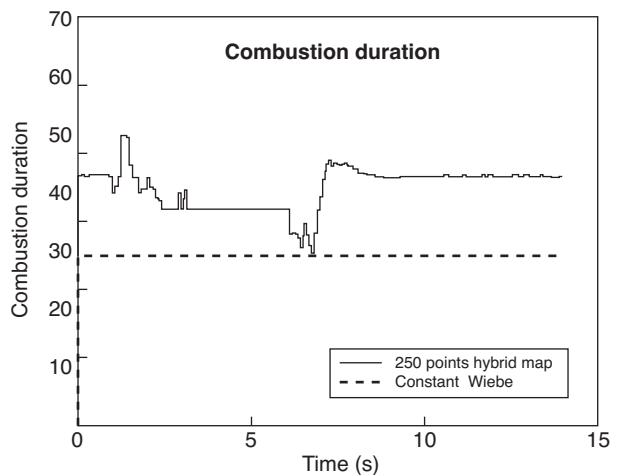
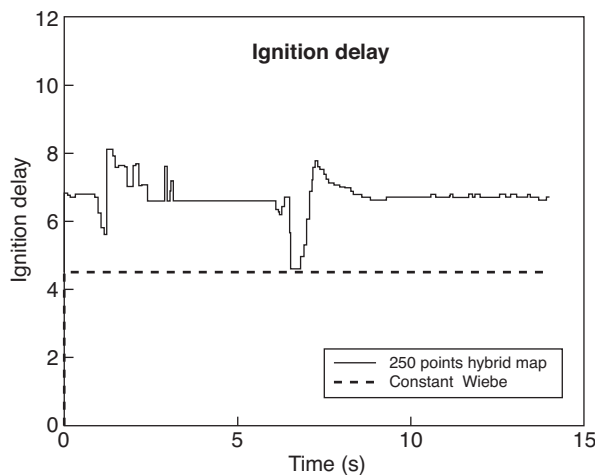


Figure 23  
Wiebe's coefficient histories.

## 5.1 Engine Configuration and Operating Conditions

The main characteristics of the turbocharged gasoline direct injection engine are presented in Table 4. Two operating points have been selected for comparison of the model results with experimental data, as given in Table 5. As explained in the previous section, the IFP-ENGINE library uses an assumption of 3 homogeneous gases while IFP-C3D uses 12 gases. The gas compatibility is ensured with the assumption that IFP-C3D burnt gases mass is equal to the IFP-ENGINE burnt gases mass. However, the IFP-ENGINE burnt gas mixture is obtained from a stoichiometric combustion and is quite different from the burnt gases mixture obtained with the 3D combustion modelling. This difference leads to a lack of accuracy. Nevertheless, as shown in Figure 24, the differences between pressure obtained with IFP-C3D and the pressure obtained with IFP-ENGINE using the 3D combustion modelling data are negligible.

The volumetric efficiency is defined as the ratio of the mass of air admitted in the cylinder to the mass that could be admitted ideally for reference conditions (25°C, 1 bar), based on the cylinder volume. The values for Points A and B are relatively low because there is valve overlap during the intake stroke (the exhaust valves are still open when the intake valves are opening).

TABLE 4  
Engine Set-up Characteristics

Engine type	RENAULT F5P
Number of cylinders	4
Bore (mm)	82.7
Stroke (mm)	83
Compression ratio	10.5:1
Connecting rod length (mm)	149.5
Engine displacement (lit.)	1.9
Turbocharger type	Single-scroll
I/O/IVC	-49° ATDC / 20° ABDC
EVO/EVC	-40° ABDC / 18° ATDC

TABLE 5  
Operating Conditions

Point	A	B
Engine speed (RPM)	2000	2000
BMEP (bar)	6	8
Throttle (%)	24.8	30.0
Volumetric efficiency	0.55	0.67
Injection timing (° CA ATDC)	-310	-290
Spark timing (° CA ATDC)	-36	-24

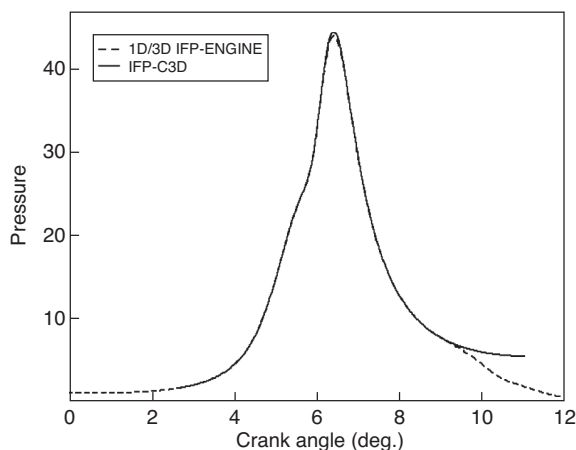


Figure 24

In-cylinder pressure 1D/3D IFP-ENGINE vs. IFP-C3D.

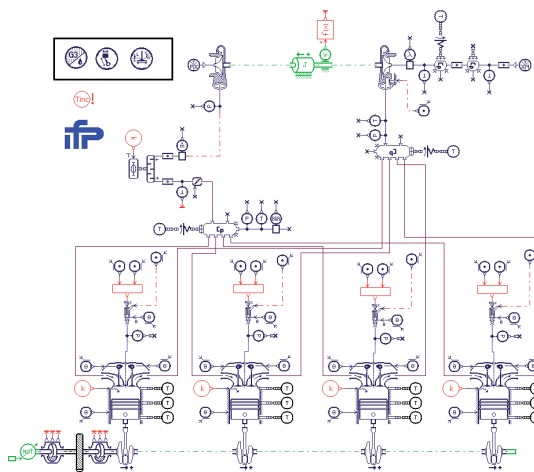


Figure 25

Turbocharged gasoline direct injection engine model.

## 5.2 Engine Model Description

The engine model diagram is presented in Figure 25. Three gases are used to model the charge: fresh air, fuel vapour, and burnt gases. The air path consists of pipes, volumes, and orifices representing the ducts manifold and piloted air throttle in the intake system. A heat exchanger is included to simulate compressed gas cooling. The engine block consists of the cylinder head with the intake and exhaust valves and four combustion chambers. The valve lift and permeability characteristics are taken into account. The turbocharger model is based on the manufacturer's maps. When the 1-D model is used for combustion, the CFM-1D model predicts the

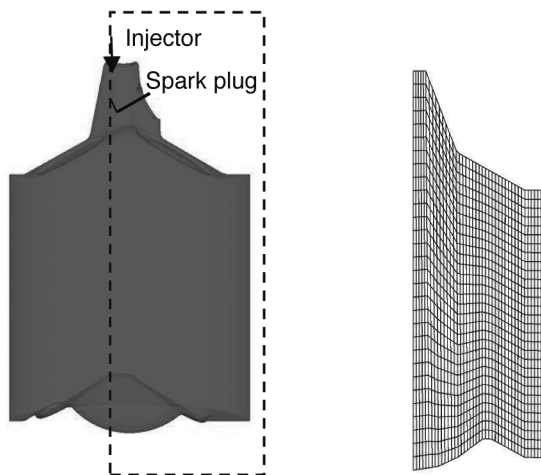


Figure 26  
Combustion chamber geometry and 2-D computational mesh, at Bottom Dead Centre (BDC).

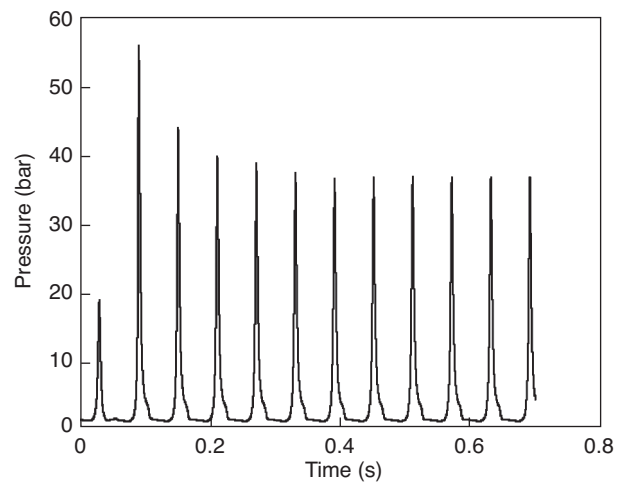


Figure 27  
Cylinder pressure until stabilization, Point A.

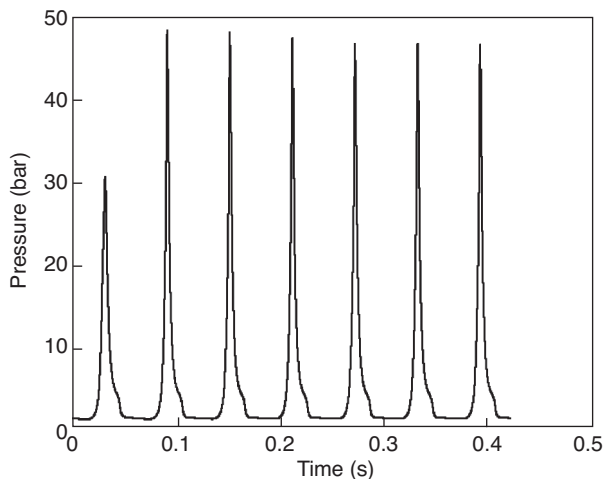


Figure 28  
Cylinder pressure until stabilization, Point B.

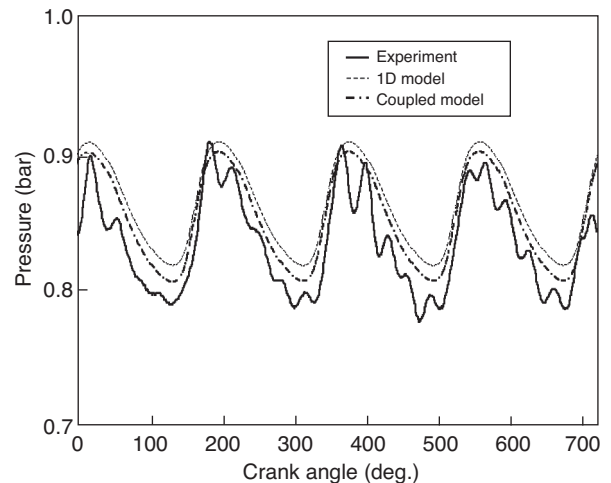


Figure 29  
Intake pressure comparison for Point A.

combustion process while Woschni's correlation is used to model heat transfer. Alternatively, the 3-D combustion model can be used, in order to provide more accurate combustion and emissions predictions.

### 5.3 3-D Model Description

The 3-D combustion simulation was performed by utilising a 2-D computational grid of the combustion chamber geometry. The actual geometry and the 2-D grid are shown in Figure 26. The fuel injector is centrally located at the top of the chamber and the spark plug is positioned just below, close to the centreline. The grid consists of 300 cells ( $20 \times 15$ ), since the goal was to demonstrate the capabilities of the model and not to obtain very detailed combustion results.

The ECFM combustion model [16] was used to predict the combustion in the cylinder. Since the model does not include valve motion and the fuel injection takes place during the intake phase, the fuel injection process is not simulated. In addition, the assumption is made that the entire mass of the fuel evaporates and the charge is homogeneous. As will be shown later, this can cause discrepancies when comparing with experimental data, particularly in the cylinder pressure during expansion and in emissions predictions.

### 5.4 Simulation Results with the Coupled Model

The coupled 1D/3D model has been evaluated against experimental data for the two points presented in Table 5. As shown in the previous section, it takes a certain number of

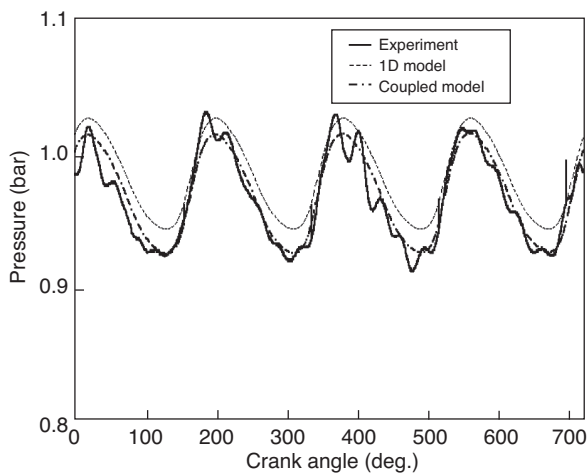


Figure 30  
Intake pressure comparison for Point B.

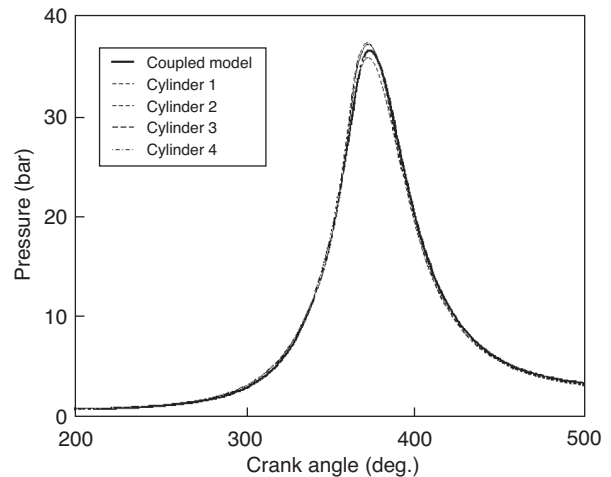


Figure 31  
Cylinder pressure comparison, Point A.

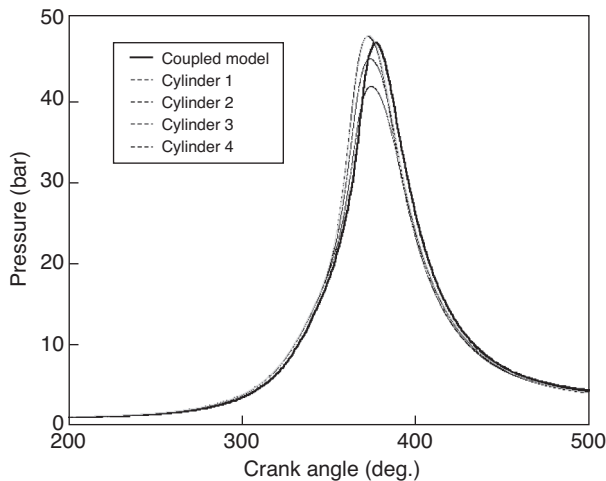


Figure 32  
Cylinder pressure comparison, Point B.

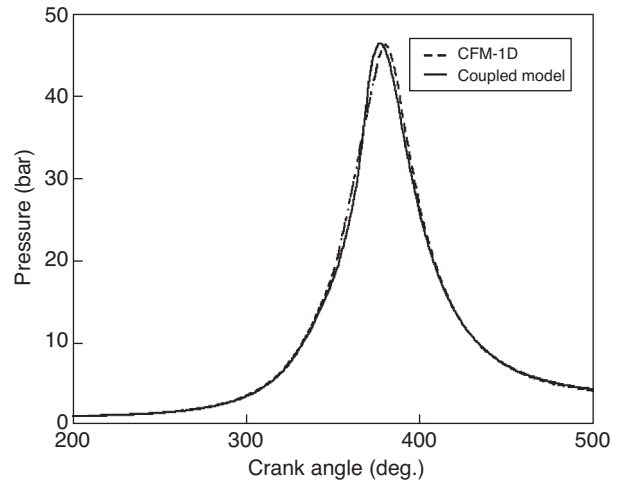


Figure 33  
Coupled vs. 1D model comparison, Point A.

cycles for the model results to stabilize. This behaviour has been observed in both cases presented here. In Figures 27 and 28, the cylinder pressure for Cylinder 1 is plotted against time. Depending on the conditions stability is achieved after 6-10 engine cycles. Once the model is stabilized, the results can be compared with experimental measurements.

The instantaneous intake pressure predictions are first presented, compared with experimental measurements in Figures 29 and 30, for Points A and B respectively. This comparison is important, in order to ensure that the correct pressure conditions are provided to the 3D combustion model. In both cases the comparison shows very good agreement between the model and experimental measurements, both in terms of phasing and in the magnitude of the fluctuation. In addition, the Coupled Model appears to have improved predictions, compared to the 1D model alone, which means

that the initial conditions for the 3D calculation will be more accurate. Higher order frequencies are not captured by the model because they are caused by the geometrical details of the pipes between the admission plenum and the valves. These details were not modelled here and a simple pipe element was used instead, in order to provide correct average values for the pressure in the intake.

Comparison of the cylinder pressure between the experiment and the coupled model is given in Figures 31 and 32 for Points A and B. Only the closed part of the cycle is shown here, it was calculated with IFP-C3D. The agreement for Point A is very good, while in Point B the combustion is initially slower and the cylinder pressure is over-predicted during the expansion stroke. The over-prediction is attributed to the fact that the fuel injection is not modelled and the mixture is assumed to be homogeneous in

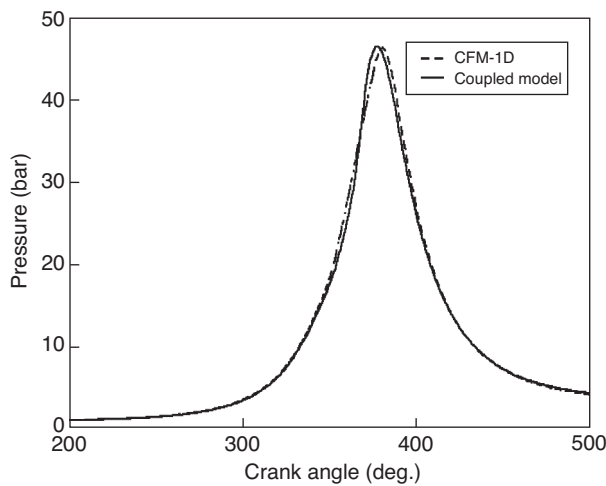


Figure 34  
Coupled vs. 1D model comparison, Point B.

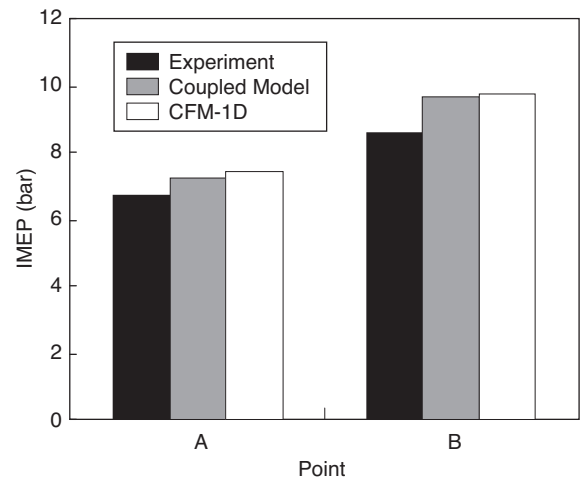


Figure 35  
Comparison of IMEP between experiment, coupled model and 1D model.

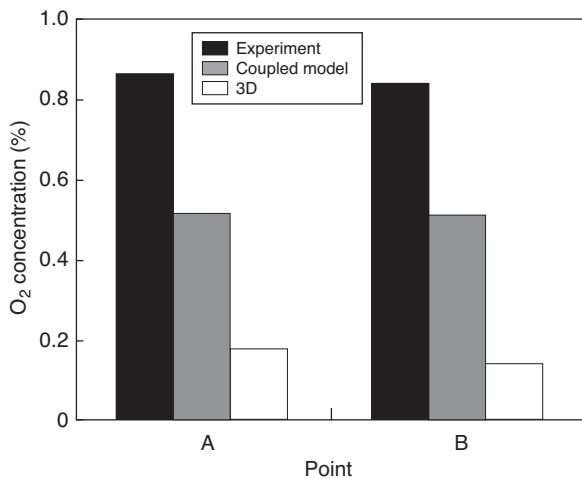


Figure 36  
O<sub>2</sub> concentration.

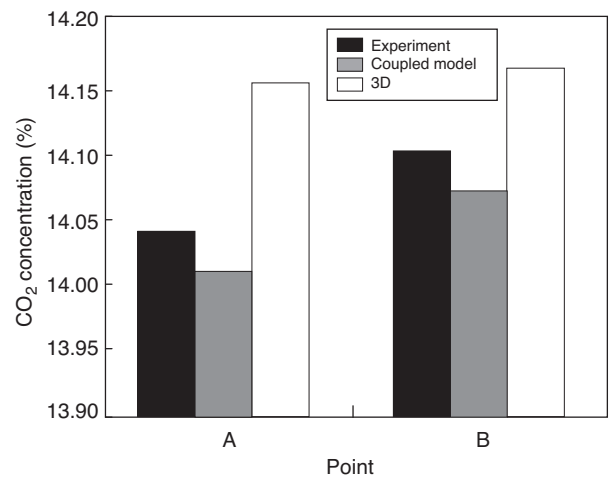


Figure 37  
CO<sub>2</sub> concentration.

the 3-D calculation. In reality, mixture stratification leads to faster initial pressure rise and results in a slightly lower pressure in expansion due to unburnt fuel in the cylinder.

The assumption of mixture homogeneity and its effect on the cylinder pressure also causes the Indicated Mean Effective Pressure (IMEP) to be somewhat higher than the experimentally measured value. However, the prediction is improved compared with the predictions of the 1D engine code, which is based on the CFM-1D model. This is demonstrated in Figures 33 and 34, showing the cylinder pressure comparison between the coupled model and the 1D, CFM-1D combustion model. The 1D model tends to predict even higher cylinder pressure during the expansion stroke, due to the homogeneity assumption. In addition, in Figure 35 the IMEP for Points A and B is shown, measured

experimentally, predicted by the coupled model and by the 1D model. Even though the computational mesh for the coupled model is very coarse and the fuel injection is not modelled, the predictions of the engine behaviour are improved, especially for Point A. It is believed that the effects of stratification, due to higher fuel quantity, are stronger in Point B, therefore the coupled model does not perform very well.

These results are encouraging, considering that in the next stages of development direct fuel injection will be added and a finer mesh will be used, which will allow for more accurate predictions. Finally, the coupled model is predictive, due to the utilisation of a 3D combustion code, as opposed to the 1D approach, where the combustion model has to be calibrated to yield proper combustion characteristics.

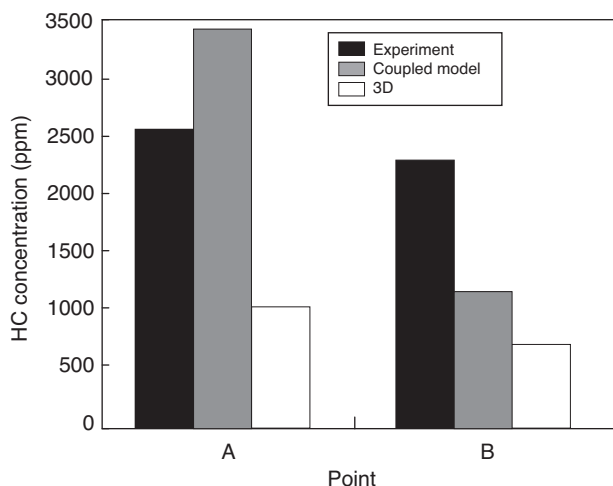


Figure 38

HC concentration.

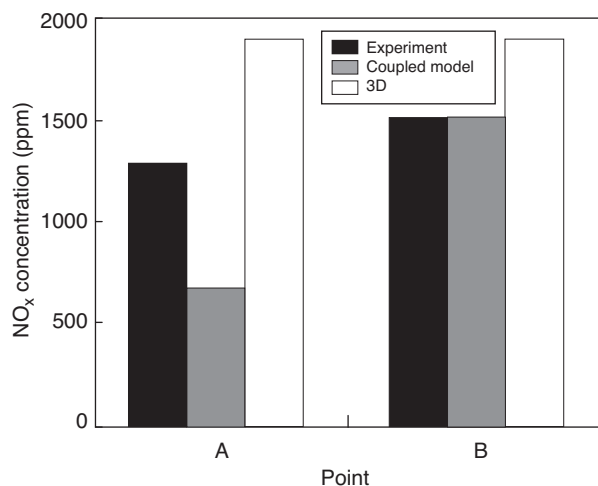


Figure 39

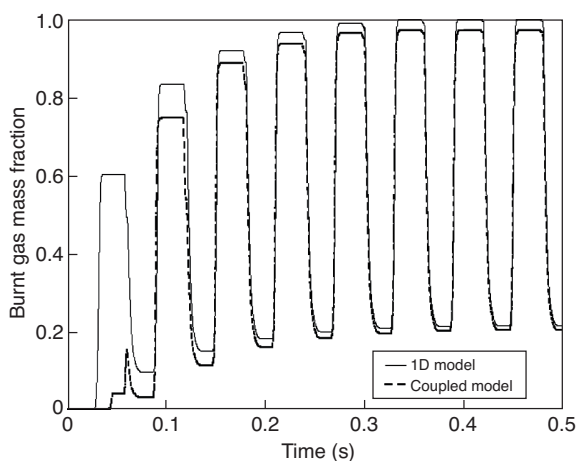
NO<sub>x</sub> concentration.

Figure 40

Burnt gas mass fraction predictions from the 1D vs. Coupled Model, Point A.

## 5.5 Emissions Predictions

One of the advantages of coupling a 1D engine simulation with a detailed 3D combustion code is the potential for more accurate emissions predictions, compared with results from the 3D code alone. The model predictions for O<sub>2</sub>, CO<sub>2</sub>, HC and NO<sub>x</sub> are shown in Figures 35-39, compared with the experimentally measured values. The results from the 3D code alone are obtained by initialising the calculations with the cylinder pressure and temperature predicted by a 1D stand-alone model.

The O<sub>2</sub> and CO<sub>2</sub> predictions from the coupled model are clearly improved, compared with the 3-D model alone. It is believed that this is a result of more accurate combustion predictions due to improved estimation of the initial conditions in the cylinder.

The unburnt HC and NO<sub>x</sub> predictions do not show a consistent trend. The HC concentration is closer to the experimental measurements, in terms of absolute values, however the drop from Point A to Point B is strongly overestimated with the coupled model. Similarly, the increase in NO<sub>x</sub> concentration is overestimated with the coupled model, even though the absolute value for Point B is very close to the experimental one. On the other hand, with the 3D code alone, the transition trends from A to B are better captured, even though the absolute values are not as close to the experimental ones. The inaccuracies observed in the unburnt HC and NO<sub>x</sub> predictions, for both models, could be attributed to the assumption of a homogeneous mixture. The mixture stratification could locally affect combustion, leading to pockets of unburnt fuel (producing unburnt HC) and areas of very high temperatures (that result in high NO<sub>x</sub> concentrations).

## 5.6 Advantages of the Coupled Model

The improvements achieved with the coupled model in IMEP predictions and pollutant concentrations can be explained by investigating the behaviour of the system and the initial conditions provided for the 3D calculation.

The classical approach to the problem would be to use a 1D simulation (with the CFM-1D combustion model) to determine the air-mass flow rate to the cylinder, the residual burnt gas fraction, as well as the initial temperature and pressure of the mixture at the IVC timing. This information could be exported and used for the IFP-C3D calculation of one engine cycle, up to the EVO timing. This method was followed for the pollutant estimates with IFP-C3D shown in Figures 35-38. However, using a 1D combustion model to estimate the initial conditions in the cylinder introduces an uncertainty and also reduces the predictability of the model. Alternatively, the coupled model approach can be used to provide more accurate initial conditions for the CFD calculation.

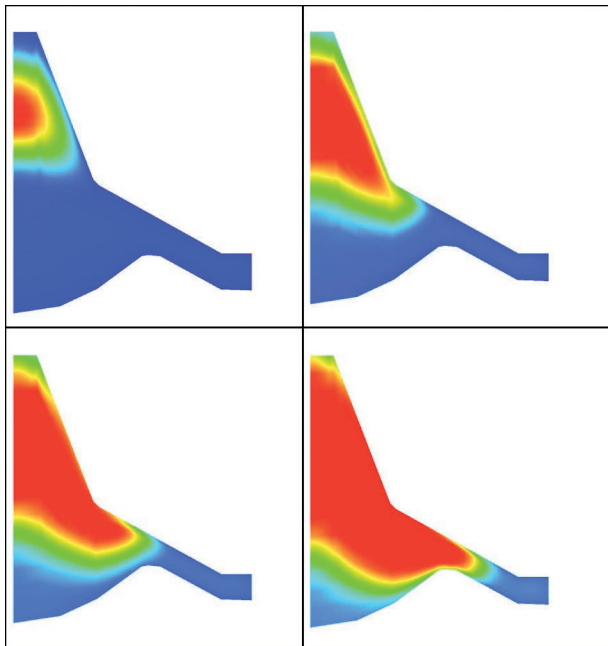


Figure 41  
Temperature contours, IFP-C3D results, Point A (CA  $-10^\circ$ ,  $-2^\circ$ ,  $+5^\circ$ ,  $+9^\circ$ ).

This is shown in Table 6, where the residual gas fraction, the initial pressure, and temperature in the cylinder are given, as predicted by the 1D model and the coupled model. In addition, in Figure 40, an example of the predicted burnt gas mass fraction in the cylinder is given, for Point A, to illustrate the differences between the 1D model predictions and the coupled model. In the 1D model the fuel is fully burnt, leading to higher residual fraction at the start of the next engine cycle. In contrast, the coupled model takes into account the incomplete burning of the fuel, resulting in eliminating some of the inaccuracies of the 1D model. This is illustrated in Figure 41, where results from the 3D combustion analysis with the 3D model are presented, showing the flame propagation in the cylinder and the low temperature areas close to the cylinder liner and inside the piston bowl.

TABLE 6

Comparison between 1D and Coupled Model predictions

	Point			
	A		B	
	Coupled model	1D model	Coupled model	1D model
Residual Gas Mass Fraction	0.205	0.216	0.133	0.135
$P_{IVC}$ (bar)	0.810	0.827	0.935	0.956
$T_{IVC}$ (K)	383	372	374	361

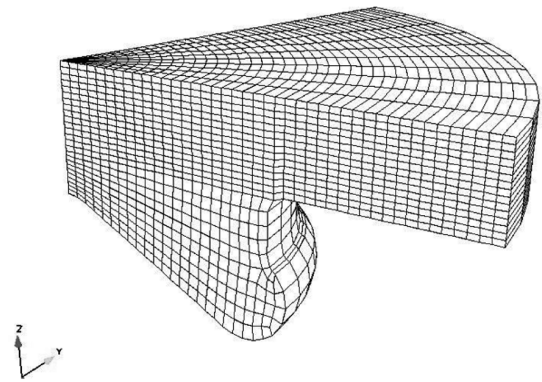


Figure 42  
Computational grid for the 72° wedge.

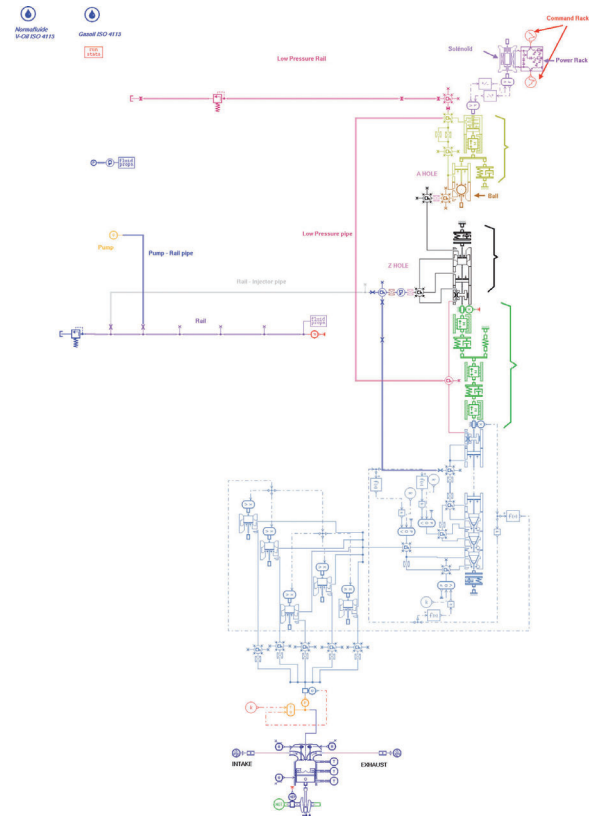


Figure 43  
1-D injector and engine simulator.

The CPU time for the coupled model is directly proportional to the number of cycles required for the stabilization of the engines' behavior. In the particular case studied here, the computational time was approximately 3 hours, as opposed to 5-10 minutes for the 1D model alone.

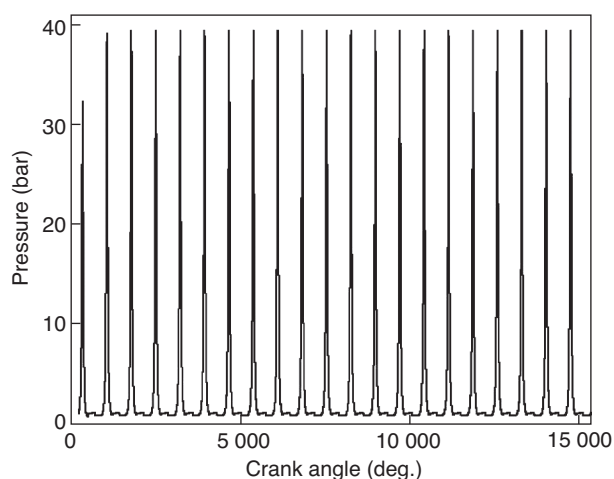
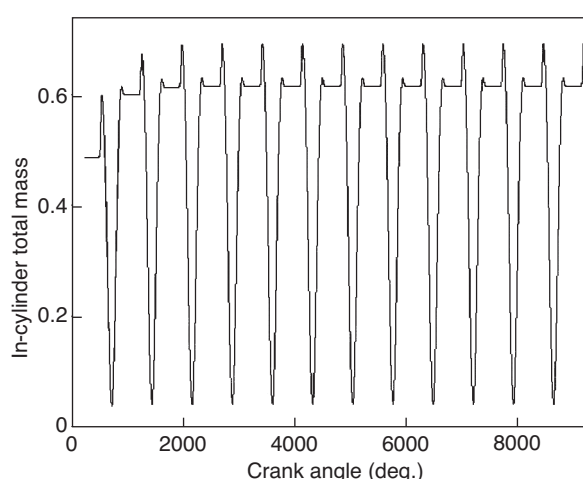


Figure 44

In-cylinder pressure and total mass histories for coupled calculation without injection.



## 6 APPLICATION ON A SINGLE-CYLINDER DIESEL ENGINE

The direct coupled method was applied on a Diesel single-cylinder direct injection diesel engine with a Bosch Common Rail injection system in order to demonstrate its capabilities. The main characteristics of the single-cylinder diesel engine are given in Table 7. A  $72^\circ$  wedge mesh is used to describe the combustion chamber in IFP-C3D which is linked with the 1-D LMS-AMESim software that includes the fuel injector and the engine simulator (cf. Fig. 43). The total CPU time for one computation on two AMD 2 GHz processors is approximately 12 hours to simulate 8 engine cycles. The CPU time is mainly spent by the 3-D calculations. First, the computational grid has been generated using the internal mesher of the code. This sector mesh contains 10 000 cells and is plotted in Figure 42. The mesh size is adapted during the cycle to optimize the node clustering during the motion of the geometry. For all operating points simulated, a first coupled calculation was performed without combustion and injection to fit the wall temperature and the air loop. Secondly, the injection system was activated and the ECFM3Z [16, 17] combustion model is used in IFP-C3D. The in-cylinder pressure predicted by the calculation without injection is plotted in Figure 45 and is in good agreement with the experimental data. This numerical result shows that thermal effect and trapped mass in the cylinder are correctly computed with IFP-ENGINE coupled with IFP-C3D.

### 6.1 Coupled 1-D Injection/3-D Combustion Calculation

The operating point selected for comparison of the model results with experimental measurements of the combustion in the cylinder is given in Table 8.

TABLE 7

Engine set-up characteristics

Engine type	Diesel Single cylinder Bowl IFP
Number of cylinders	1
Bore (mm)	87
Stroke (mm)	92
Compression ratio (-)	14.7
Connecting rod length (mm)	149.9
Engine displacement (cm <sup>3</sup> )	546.9
IVO/IVC	42° BTDC/124° BTDC
EVO/EVC	146° ATDC/43° ATDC

TABLE 8

Engine operating conditions

Engine speed (RPM)	1500
IMEP (bar)	3.44
Injection pressure (bar)	900
Inj. timing (° CA ATDC)	Pilot: $-17^\circ$ Main: $-5^\circ$
Fuel volume injected (mm <sup>3</sup> )	3.9-12.80

Figure 46 shows an injection flow rate, as measured experimentally for the case of a pilot injection at  $-17^\circ$  with a main injection at  $-5^\circ$ . For this injection timing, the injection system predict with accuracy the mass of fuel injected and the injection rate. However, the model cannot predict a wave phenomena in the main injection that explains the error in the prediction of the injected mass. This wave phenomenon is observed in all injection events and we did not manage to understand this physical process to avoid this lack of accuracy.

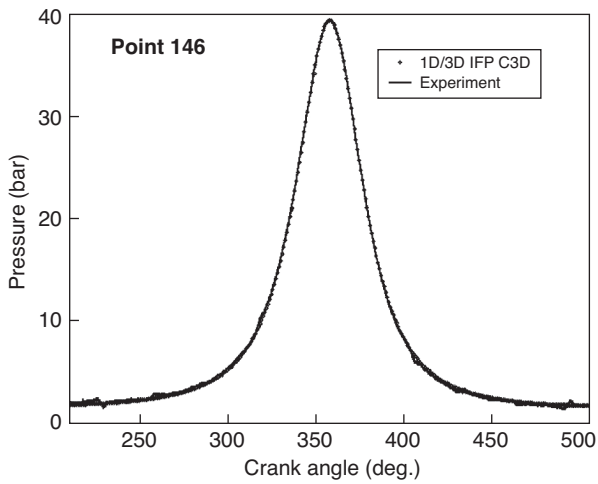


Figure 45  
In-cylinder pressure (bar) calculated with the coupled system without fuel injection.

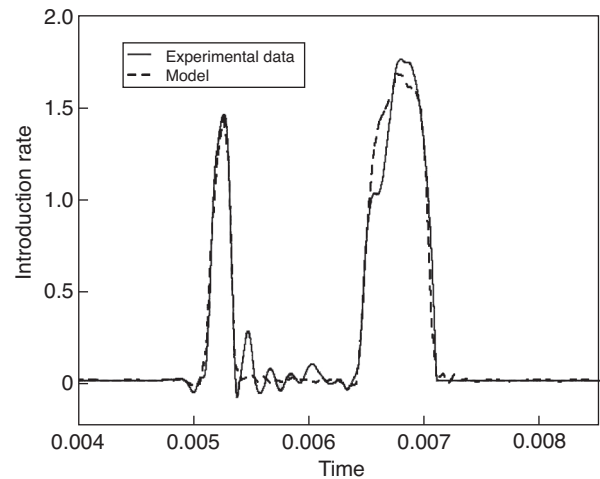


Figure 46  
Injection rate modeled vs. Experimental data for dwell = 12°.

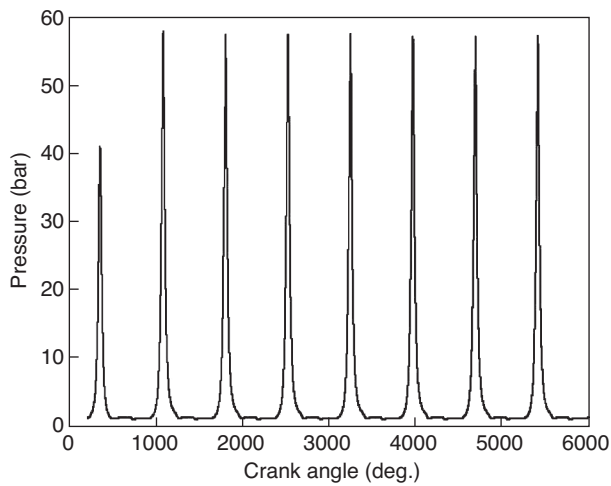


Figure 47  
In-cylinder pressure history.

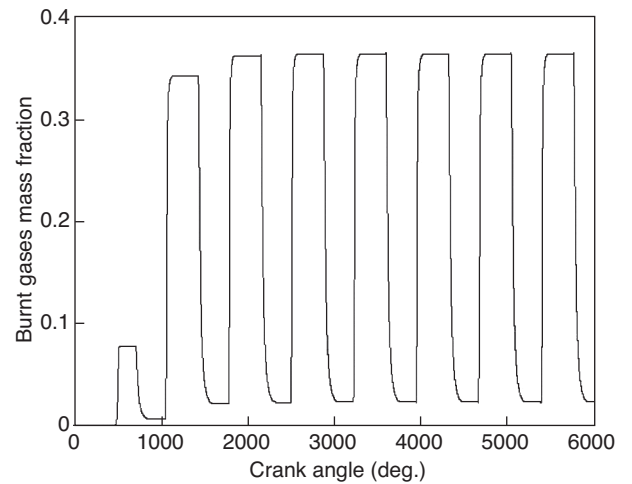


Figure 48  
Burnt gases mass fraction history.

As described before, a first calculation has been done to fit the engine system parameter. The system stabilized after approximately four engine cycles. The intake pressure was set to 0.1108 MPa and the exhaust pressure to 0.1208 MPa (experimental plenum pressure). The wall temperature was set to 450 K for the piston and the cylinder wall and to 370 K for the cylinder head. In Figure 44, the in-cylinder pressure and total mass histories are presented and attest that the dynamic system has converged. The in-cylinder predicted by the calculation without injection is plotted in Figure 45 and is in good agreement with experimental data. This result shows that thermal effect and mass in the cylinder are correctly computed with IFP-ENGINE coupled with IFP-C3D. The next step is now to inject fuel into the system to simulate the 3-D combustion process with the IFP-C3D combustion code.

In a second step, the full system was simulated. For this calculation, all the initial parameters needed by IFP-C3D to compute the combustion were automatically computed and received from the injector simulator and the engine system simulator. In fact, the 1-D/3-D calculation is like a typical system simulation. Injection command is filled as the experimental test in the system and the calculation can be run. For engineers used to make 3-D calculations, this coupled way avoids the difficult task of fitting the initial parameters and is really a great advantage. However, the coupled calculation needs more CPU times to stabilize the dynamic system. As seen in Figures 47 and 48, the system converged after five engine cycles. Figure 49 shows the comparison of the in-cylinder pressure predicted by the coupled simulation. The coupled simulation result is in good agreement with the experimental pressure. As

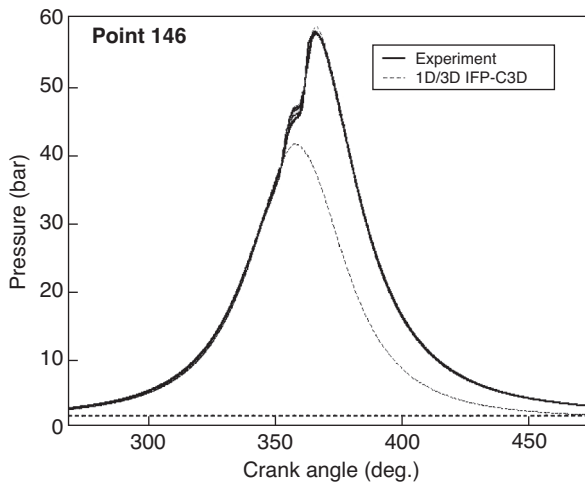


Figure 49

In-cylinder pressure history vs. Experiment data for dwell = 12° (8 cycles plotted with a crank angle modulo 720°).

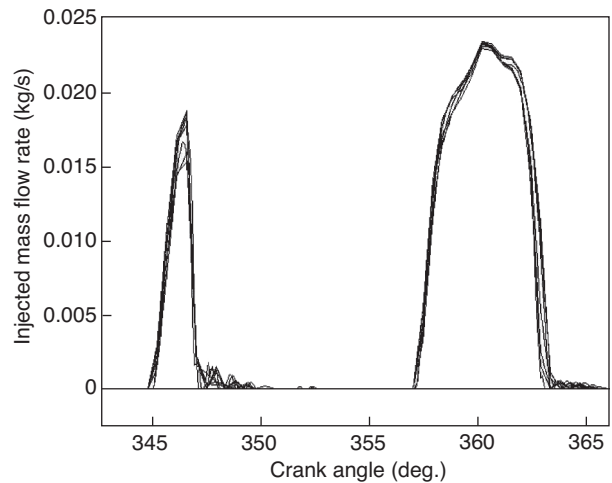


Figure 50

Injected mass flow rate history (8 cycles plotted with a crank angle modulo 720°).

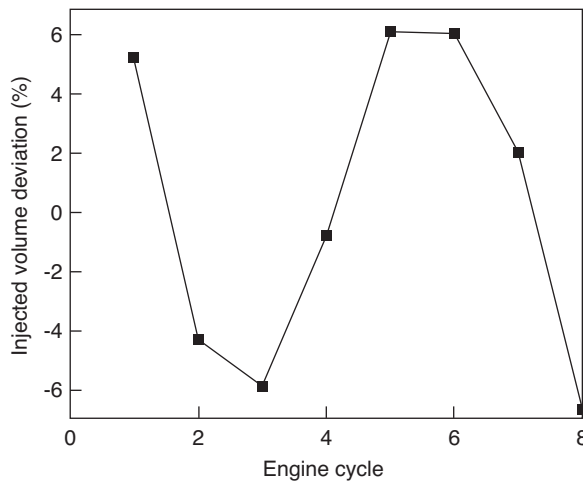


Figure 51

Injected volume deviation history (%).

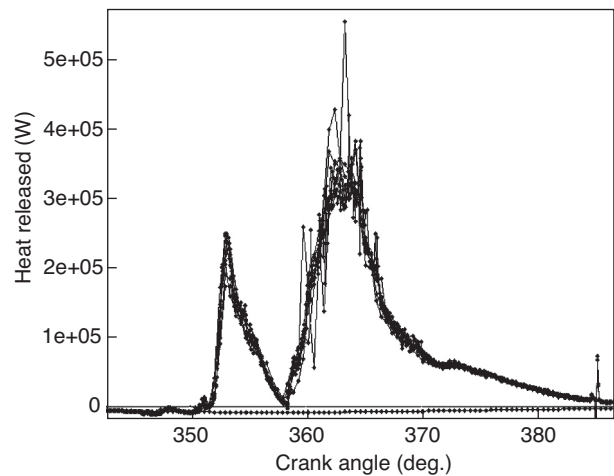


Figure 52

Combustion heat released time history (8 cycles plotted with a crank angle modulo 720°).

seen in this graph, a small variation of the pressure can be observed and is due to the fluctuation of the in-cylinder mass and of the mass fraction of the burnt gases but is also due to the injected mass flow rate fluctuations. Figure 50 shows the injected mass flow rate history using a crank angle modulo 720° abscissa and we can notice that the pilot injection and the main injection mass flow rate are influenced by the pressure in-cylinder history. The fuel mass predicted by the injector simulator for each engine cycle varies between  $\pm 6\%$  in comparison with the average value (see Fig. 51). The injected volumes of the pilot and of the main injection have a cycle/cycle variation behavior. The experimental data gives for this operating condition a rate of IMEP instability equal to 1.7% that do not fit with this large variation. In a first step,

because of a lack of experimental data to validate this variation and eventually to fit the 1-D injector model, the coupled calculation used a fixed mass of fuel for each engine cycle given by the average of injected mass values. IFP-C3D uses the instantaneous injection rate given by the 1-D injector model to model the fuel spray with this average mass. Figure 52 plots the combustion heat released and we can notice the two local extremum representing the pilot injection and the main injection combustions. Fluctuations in the heat mass released are larger and attest that small fluctuations may have a larger impact on 3-D calculation prediction and in particular for pollutant predictions. Obviously, the variation of injected fuel mass may have a major effect on 3-D combustion calculation. The 1-D/3-D coupled system is able

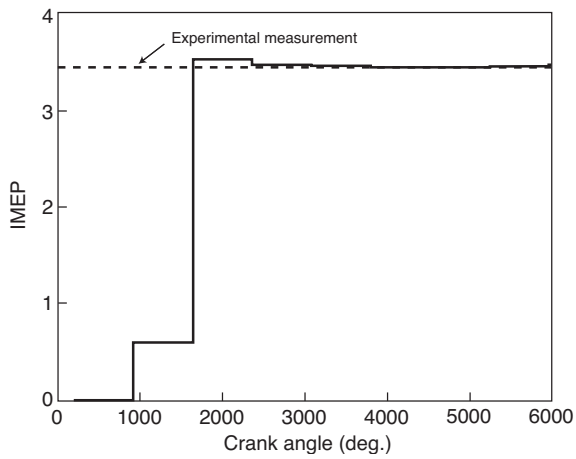


Figure 53  
IMEP history vs. experiment.

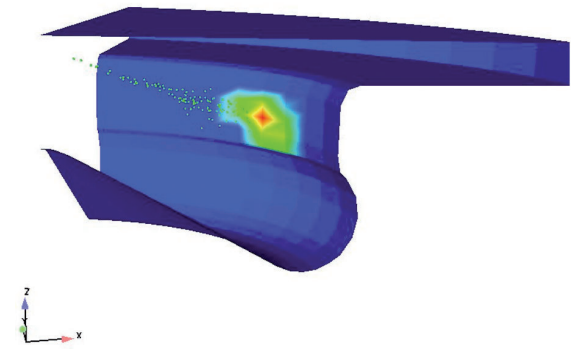


Figure 54  
View of liquid film thickness of the 3-D calculation during the pilot injection. A liquid film formation during the pilot injection can be observed.

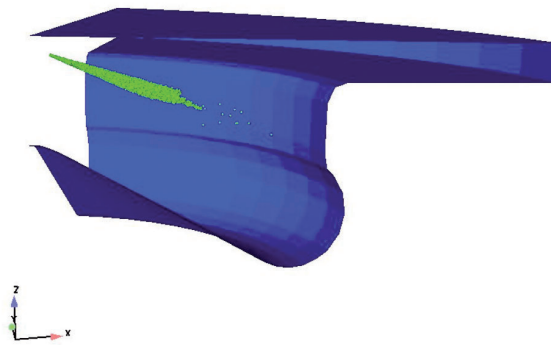


Figure 55  
View of liquid film thickness of the 3-D calculation during the main injection. Liquid fuel droplets evaporate before reaching the cylinder wall.

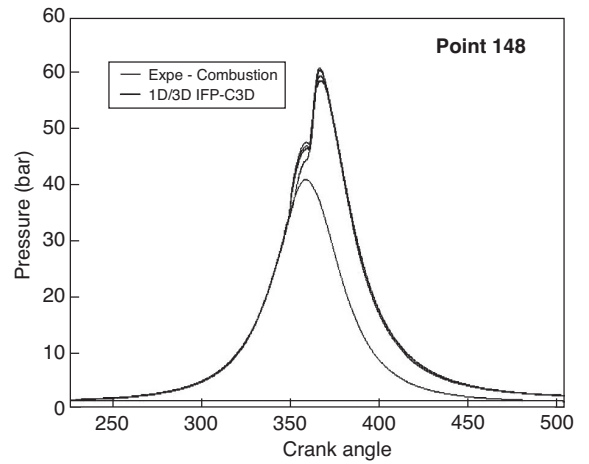


Figure 56  
In-cylinder pressure (bar) for dwell = 16°.

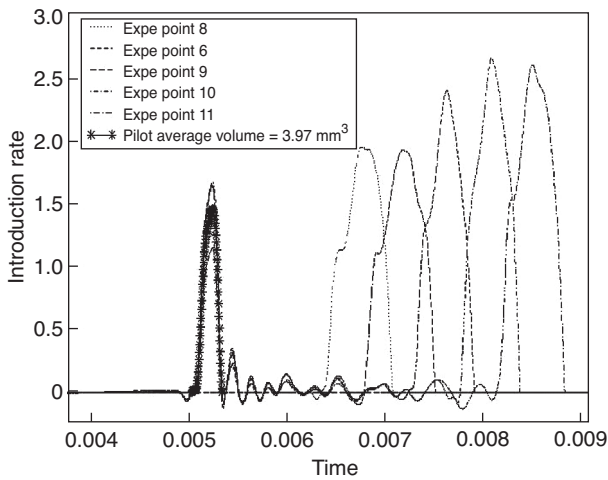


Figure 57  
Experimental injection rate.

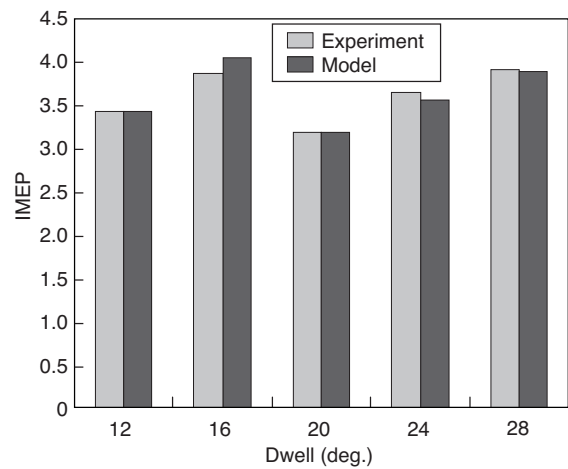


Figure 58  
Calculation vs. experimental measurements of IMEP and injected mass as a function of the dwell angle.

to predict the average experimental IMEP plotted in Figure 53. As seen in this figure, the dynamic system converges after few cycles to the experimental IMEP. Figures 54 and 55 present 3-D views of the combustion chamber. For these multi-injection events, the spray particles impact the cylinder wall during the pilot injection. These pictures correspond to the last engine cycle during the pilot injection and the main injection.

## 6.2 Effect of Injection Parameters on Combustion

The coupled model was tested by comparing model predictions with experimental measurements. The injection timing of the pilot injection in the single-cylinder engine was varied, in order to study the effect on combustion. The experimental injection flow rate for all operating points are plotted in Figure 57. In Figure 58 the Indicated Mean Effective Pressure (IMEP) is shown for 5 different injection timings that leads to different injected mass (Fig. 59). The main injection was held constant at  $-5^\circ$  ATDC, while the pilot was varied from  $-17^\circ$  to  $-33^\circ$  ATDC. The coupled model is able to predict the IMEP variation when the pilot injection timing is varying. The injection rate for each operating condition is automatically computed by the injector model and IFP-C3D computes the combustion using ENGINE results for the trapped mass and burnt gases mass fraction. Actually, the IMEP is mainly dependent of the injected mass and on the prediction of the injector model. However, spray impact has been noticed for late pilot injection timing which can explain IMEP variation. Figure 56 presents the pressure computed for a delay of  $16^\circ$  between pilot and main injection. The 1-D injector model needs to be tested more intensively with experimental data to improve the numerical results and to understand the cycle/cycle dynamic behavior.

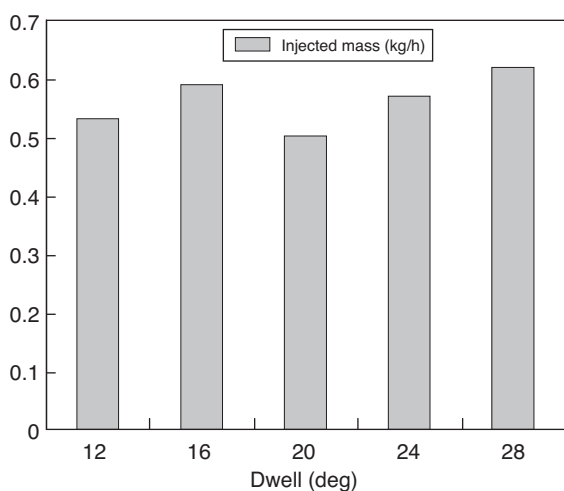


Figure 59  
Experimental fuel flow rate.

## CONCLUSION

This paper describes a new methodology that involved 1-D simulation, 0-D air loop simulation and 3-D combustion calculation coupled to simulate the full engine system with a predictive combustion modelling. This multi-scale simulation enables us to compute 3-D detailed combustion using accurate and dynamic conditions given by the 0-D air-loop model and 1-D injection model. The first coupled approach which is mainly dedicated to the simulation of engine transient operating conditions, consists in using, in IFP-ENGINE models, numerical combustion maps automatically generated with IFP-C3D. The use of a 3D combustion code such as IFP-C3D to compute the maps, enables the user to get valuable combustion data even for operating conditions that are not available from experiments. The validity and efficiency of the method are demonstrated by numerical tests and comparisons with test bed results obtained on a turbocharged gasoline engine. The second approach based on a direct temporal coupling can be used to make easier 3-D calculations but also to avoid the difficult task of defining all initial conditions needed by the 3-D calculation. Indeed, more than one cycle is needed to converge to a stabilized solution and a coupled simulation needs at least five engine cycles. This return calculation time may decrease with more than two processors for parallel calculation and with new processor development (high speed multi-core processor, high number of processors per node). Moreover, using a heterogeneous parallel grid computer helps to manage multi-scale calculation and may also reduce the CPU cost. This coupling algorithm was used in a Diesel direct injection single-cylinder engine on a variety of injection conditions. Numerical results are in good agreement with experimental results. This coupling algorithm can be used to simulate 3-D cycle/cycle variation due to fluctuation in the injection system or in the air-loop system. Moreover, 3-D calculations can compute pollutant emissions which can be used by the 1-D engine system model to predict the engine pollutant emissions. In the future, the engine system will be modified to add EGR loop and to test coupled calculation for operating conditions with EGR.

## REFERENCES

- 1 Ficarella, Laforgia D., Landriscina V. (1999) Evaluation of Instability Phenomena in a Common Rail Injection System for High Speed Diesel Engines, *SAE Technical Paper Series* 1999-01-0192.
- 2 Desantes J.M., Arrègle J., Rodríguez P.J. (1999) Computational Model for Simulation of Diesel Injection Systems, *SAE Technical Paper Series* 1999-01-0915.
- 3 Han J.-S., Wang T.C., Lai M.-C., Henein N.A., Harrington D.L., Pinson J., Miles P. (2000) Dynamics of Multiple-Injection Fuel Sprays in a Small-bore HSDI Diesel Engine, *SAE Technical Paper Series* 2000-01-1256.
- 4 Bianchi G.M., Falfari S., Pelloni P., Kong S.-C., Reitz R.D. (2002) Numerical Analysis of High pressure Fast-Response

- Common Rail Injector Dynamics, *SAE Technical Paper Series* 2002-01-0213.
- 5 Bianchi G.M., Falfari S., Pelloni P., Filicori F., Milani M. (2002) A Numerical and Experimental Study Towards Possible Improvement of Common Rail Injectors, *SAE Technical Paper Series* 2002-01-0500.
- 6 Zhong L., Singh I.P., Han J., Lai M.-C., Henein N.A., Bryzik W. (2003) Effect of Cycle-to-Cycle Variation in the Injection Pressure in a Common Rail Injection System on Engine Performance, *SAE Technical Paper Series* 2003-01-0699.
- 7 Sinclair R., Strauss T., Schindler P. (2000) Code Coupling, a New Approach to Enhance CFD Analysis of Engines, *SAE Technical Paper Series* 2000-01-0660.
- 8 Borghi M., Mattarelli E., Montorsi L. (2001) Integration of 3-D-CFD and Engine Cycle Simulations: Application to an Intake Plenum, *SAE Technical Paper Series* 2001-01-2512.
- 9 Riegler U.G., Bargende M. (2002) Direct Coupled 1-D/3-D-CFD-Computation (GT-Power/Star-CD) of the Flow in the Switch-Over Intake System of an 8-Cylinder SI Engine with External Exhaust Gas Recirculation, *SAE Technical Paper Series* 2002-01-0901.
- 10 Wehr D., Huurdeman B., Spennemann A. (2002) EGR – A Challenge for Modern Plastic Intake Manifolds, *SAE Technical Paper Series* 2002-01-0902.
- 11 Bohbot J., Chryssakis C., Marjorie M. (2006) Simulation of a 4-Cylinder Turbocharged Gasoline Direct Injection Engine Using a Direct Temporal Coupling Between a 1-D Simulation Software and a 3-D Combustion Code, *SAE Technical Paper Series* 2006-01-3263.
- 12 Menegazzi P., Aubret P., Vernhes P.-L. (2004) Conventional and Hybrid Vehicle Emission, Fuel Economy and Performance Analysis System Simulation, *FISITA 2004*, 23-27 May, Barcelona, Spain.
- 13 Zolver M., Benkenida A., Bohbot J., Klahr D., Réveillé B. (2004) CFD Tools at IFP for HCCI Engine Simulations, *14th International Multidimensional Engine Modeling User's Group Meeting at the SAE 2004*, March 2004, Detroit, USA.
- 14 Zolver M., Klahr D., Bohbot J., Laget O., Torres A. (2003) Reactive CFD in Engines with a New Unstructured Parallel Solver, *Oil Gas Sci. Technol.* **58**, 33-46.
- 15 Zolver M., Bohbot J., Klahr D., Torres A. (2003) An Unstructured Parallel Solver for Multi-Phase and Reactive Flows in Internal Combustion Engines, *Parallel CFD 2003*, May 2003, Moscow.
- 16 Colin O., Benkenida A., Angelberger C. (2003) A 3-D Modeling of Mixing, Ignition and Combustion Phenomena in Highly Stratified Gasoline Engines, *Oil Gas Sci. Technol.* **58**, 47-62.
- 17 Colin O., Benkenida A. (2004) The 3-Zones Extended Coherent Flame Model (ECFM3Z) for Computing Premixed Diffusion Combustion, *Oil Gas Sci. Technol.* **59**, 6, 593-609.
- 18 Colin O., Pires da Cruz A., Jay S. (2004) Detailed chemistry based auto-ignition model including low temperature phenomena applied to 3-D engine calculations, *30th Symposium (International) on Combustion*, The Combustion Institute.
- 19 Han Z., Reitz R.D. (1995) Multidimensional Modeling of Internal Combustion Engines Using RNG k- $\epsilon$  Models, *Combust. Sci. Technol.* **106**, 206-280.
- 20 Lafossas FA, Colin O. *et al.* (2005) Application of a new 1-D combustion model to gasoline transient engine operation, *SAE Technical Paper Series* 2005-01-2107.
- 21 Barba C., Burkhardt C., Boulouchos K., Bargende M. (2000) A phenomenological combustion model for heat release rate prediction in high speed DI Diesel engines with common-rail injection, *SAE Technical Paper* 2000-01-2933.
- 22 Vibe I.I. (1956) Semi-empirical expression for combustion rate in engines, *Proceedings of Conference on piston engines*, USSR Academy of Sciences, Moscow, pp. 186-191.
- 23 Woschni G. (1967) Universally Applicable Equation for the Instantaneous Heat Transfer Coefficient in the Internal Combustion Engine, *SAE paper* 670931, *SAE Trans.* **76**.
- 24 Heywood J.B. (1988) *Internal Combustion Engine Fundamentals*, McGraw Hill.
- 25 Chmela F., Orthaber G. (1999) Rate of Heat Release Prediction for Direct Injection Diesel Engines Based on Purely Mixing Controlled Combustion, *SAE Technical Paper* 1999-01-0186.

Final manuscript received in September 2008  
Published online in June 2009